AD723821

NOLTR 71-25

VERTICAL WATER ENTRY OF CONES

By
John L. Baldwin

DDC
RECEIVED
MAY 28 1971
A

11 February 1971

NOL

NAVAL ORDNANCE LABORATORY, WHITE OAK, SILVER SPRING, MARYLAND

NOLTR 71-25

ATTENTION

This document has been approved for public release and sale, its distribution is unlimited.

Reproduced by
NATIONAL TECHNICAL
INFORMATION SERVICE
Springfield Va 22151

65

UNCLASSIFIED

Security Classification

DOCUMENT CONTROL DATA - R & D

(Security classification of title, body of abstract and indexing annotation must be entered when the overall report is classified)

1. ORIGINATING ACTIVITY (Corporate author) Naval Ordnance Laboratory White Oak, Silver Spring, Maryland 20910	2a. REPORT SECURITY CLASSIFICATION UNCLASSIFIED 2b. GROUP N/A

3. REPORT TITLE

VERTICAL WATER ENTRY OF CONES

4. DESCRIPTIVE NOTES (Type of report and inclusive dates)

5. AUTHOR(S) (First name, middle initial, last name)

John L. Baldwin, Jr.

6. REPORT DATE 11 February 1971	7a. TOTAL NO. OF PAGES 65	7b. NO. OF REFS 9
8a. CONTRACT OR GRANT NO. b. PROJECT NO ORD 035B 001/UR1 09 01 01 c. d.	9a. ORIGINATOR'S REPORT NUMBER(S) NOLTR 71-25 9b. OTHER REPORT NO(S) (Any other numbers that may be assigned this report)	

10. DISTRIBUTION STATEMENT

This document has been approved for public release and sale, its distribution is unlimited.

11. SUPPLEMENTARY NOTES	12. SPONSORING MILITARY ACTIVITY Naval Ordnance Systems Command Washington, D.C.

13. ABSTRACT

An experimental investigation of the vertical water-entry deceleration of various cone nose shapes, and a data-reduction method for the resulting information are described. Total drag coefficient, and added mass coefficient are determined as functions of penetration distance. These functions are shown to be independent of entry velocity and model mass over a wide range of test conditions. A method of predicting the accelerations experienced by the vertical water entry of an arbitrary cone is described.

DD FORM 1 NOV 65 1473 (PAGE 1)

S/N 0101-807-6801

UNCLASSIFIED

Security Classification

UNCLASSIFIED
Security Classification

14 KEY WORDS	LINK A ROLE	LINK A WT	LINK B ROLE	LINK B WT	LINK C ROLE	LINK C WT
Cones						
Water Entry						
Vertical						
Drag						
Added Mass						

DD FORM 1 NOV 65 1473 (BACK)
(PAGE 2)

UNCLASSIFIED
Security Classification

VERTICAL WATER ENTRY OF CONES

Prepared by:
John L. Baldwin

ABSTRACT: An experimental investigation of the vertical water-entry deceleration of various cone nose shapes, and a data-reduction method for the resulting information are described. Total drag coefficient, and added mass coefficient are determined as functions of penetration distance. These functions are shown to be independent of entry velocity and model mass over a wide range of test conditions. A method of predicting the accelerations experienced by the vertical water entry of an arbitrary cone is described.

NAVAL ORDNANCE LABORATORY
SILVER SPRING, MARYLAND

NOLTR 71-25 11 February 1971

VERTICAL WATER ENTRY OF CONES

This report is one result of the continuing effort of the Naval Ordnance Laboratory in the understanding of water-entry phenomena. The research reported herein was supported entirely by the Naval Ordnance Systems Command, Codes 035 and 054.

GEORGE G. BALL
Captain, USN
Commander

A. E. Seigel

A. E. SEIGEL
By direction

CONTENTS

	Page
INTRODUCTION	1
TEST PROCEDURE	1
RANGE OF VARIABLES TESTED	6
DATA REDUCTION	6
RESULTS AND CONCLUSIONS	12
APPLICATION OF RESULTS	21
RECOMMENDATIONS	22
REFERENCES	23
APPENDIX A	A-1
APPENDIX B	B-1
APPENDIX C	C-1
APPENDIX D	D-1

ILLUSTRATIONS

Figure	Title	Page
1	Hydroballistics Pilot Tank	2
2	Test Equipment Schematic	3
3	Sample of Test Data	5
4	Distribution of Variables	7
5	Force Model vs Depth	11
6	Measured Depth Compared to Computer Depth	11
7	Maximum Total Drag Coefficient vs Total Cone Angle	15
8	Penetration Ratio vs Total Cone Angle	16
9	Total Added Mass Constant vs Total Cone Angle	16
10	Correction of Total Added Mass Constant vs Total Cone Angle	18
11	Added Mass Associated with Maximum Drag Coefficient vs Cone Angle	18
12	Added Mass Constant vs Total Cone Angle	19
13	Added Mass vs Depth	20
A-1	Original Data - Shots 1904, 1916	A-3
A-2	Original Data - Shots 1893, 1675	A-4
A-3	Original Data - Shots 2337, 1687	A-5
A-4	Original Data - Shots 2429, 1654	A-6
A-5	Original Data - Shots 2431, 2449	A-7
A-6	Original Data - Shots 1981, 2032	A-8
A-7	Original Data - Shots 2061, 21404	A-9
A-8	Original Data - Shots 2023, 2026	A-10
B-1	Drag Plate Model - 10, 15, and 20° Cone Angles	B-2
B-2	Lightweight 20° Model	B-3
B-3	Normal Weight Models 20 through 140° Cone Angles	B-4
B-4	Glint Models 45, 60, and 90° Cone Angles	B-5
B-5	Lightweight Models 90, 120, and 140° Cone Angles	B-6
C-1	Average Total Drag Coefficient and Added Mass vs Depth for 45° Cones	C-9

CONTENTS (CONT.)

Figure	Title	Page
C-2	Average Total Drag Coefficient and Added Mass vs Depth for 60° Cones	C-12
C-3	Average Total Drag Coefficient and Added Mass vs Depth for 90° Cones	C-15
C-4	Average Total Drag Coefficient and Added Mass vs Depth for 120° Cones	C-18
C-5	Average Total Drag Coefficient and Added Mass vs Depth for 140° Cones	C-21

TABLES

Table	Title	Page
1	Steady State-Drag Coefficient	8
2	Comparison of Measured Depth and Computer Depth	12
3	Maximum Drag Coefficients for Various Model Weights	13
A-1	Numerical Constants	A-2
C-1	Summary of Cone Data	C-2
C-2	10-Degree Total-Angle Cones	C-3
C-3	20-Degree Total-Angle Cones	C-4
C-4	30-Degree Total-Angle Cones	C-5
C-5	Total Drag Coefficient and Added Mass 10-, 15-, 20- and 30-Degree Total-Angle Cones	C-6
C-6	45-Degree Total-Angle Cones	C-7
C-7	Total Drag Coefficient and Added Mass for 45-Degree Cone	C-8
C-8	60-Degree Total-Angle Cones	C-10
C-9	Total Drag Coefficient and Added Mass for 60-Degree Cone	C-11
C-10	90-Degree Total-Angle Cones	C-13
C-11	Total Drag Coefficient and Added Mass for 90-Degree Cone	C-14
C-12	120-Degree Total-Angle Cones	C-16
C-13	Total Drag Coefficient and Added Mass for 120-Degree Cone	C-17
C-14	140-Degree Total-Angle Cones	C-19
C-15	Total Drag Coefficient and Added Mass for 140-Degree Cone	C-20

LIST OF SYMBOLS

a	acceleration
A	area to which drag coefficients are related
A_b	base area of the cone
B	buoyancy
C_d	total drag coefficient
C_{di}	instantaneous drag coefficient
C_{ds}	steady state drag coefficient
C_f	friction drag coefficient
F	axial force
g	acceleration of gravity
h	penetration ratio
k	added mass constant
L	cone length
m	added mass
M	mass of model
R	base radius of cone
RC	resistance-capacitance time constant
R_i	instantaneous radius
S	depth (distance traveled after impact)
t	time from impact
U	instantaneous velocity
U_o	model velocity at impact

INTRODUCTION

Considerable effort has been devoted to the solution of the water-entry problem as shown in reference 1, which lists 135 reports on this subject. The theories presented in prior work are in serious conflict, even for simple shapes such as cones. For example, Hoover and Reardon, reference 2, use the assumption attributed to von Karman that the amount of added mass gained during impact depends only upon the size of the body and not at all upon the nose shape, while Shiffman and Spencer, reference 3, show that for cone-shaped bodies, the amount of added mass is a widely varying function of cone angle. This confusion of theories has been compounded by a relative lack of experimental data, with the exception of the work of Watanabe, reference 4; Majer, reference 5; and Mosteller, reference 6. These early (prior to 1960) experimenters, however, were severely restricted by available instrumentation which limited impact velocity and/or configuration, and inadequate computing facilities which complicated the data analysis and essentially limited the practical number of tests conducted. During the last ten years, these difficulties have to a large extent been eliminated. Furthermore, facilities such as the large Hydroballistics Facility and associate Pilot Tank at the Naval Ordnance Laboratory have been constructed specifically for the study of water-entry phenomena. A program was initiated at NOL in 1967 to obtain basic vertical water-impact acceleration data for conical shapes and to reduce the results to a simple form for engineering applications. The conical shape was chosen because of similitude considerations. These indicated that for any one cone angle the drag coefficient, based upon the area intersected by the original water surface, remained constant; and that a linear relationship exists between the distance penetrated and the effective distance penetrated.

TEST PROCEDURE

All experiments were conducted in a similar manner with the majority of the tests being made in the Pilot Hydroballistics Facility at the Naval Ordnance Laboratory (Fig. 1). The model, containing a single axially mounted crystal accelerometer, was launched from an air gun (velocity, 30 feet per second and higher) or dropped through a tube, such that normal impact with the surface of the water resulted. A cable (trailing wire) connected the accelerometer within the model to fixed electronics. The final output of the gage was photographically recorded from a CR oscilloscope. As the model neared the water surface, a trigger screen was interrupted, causing a microsecond strobe lamp to produce three flashes equally spaced in time, thereby exposing

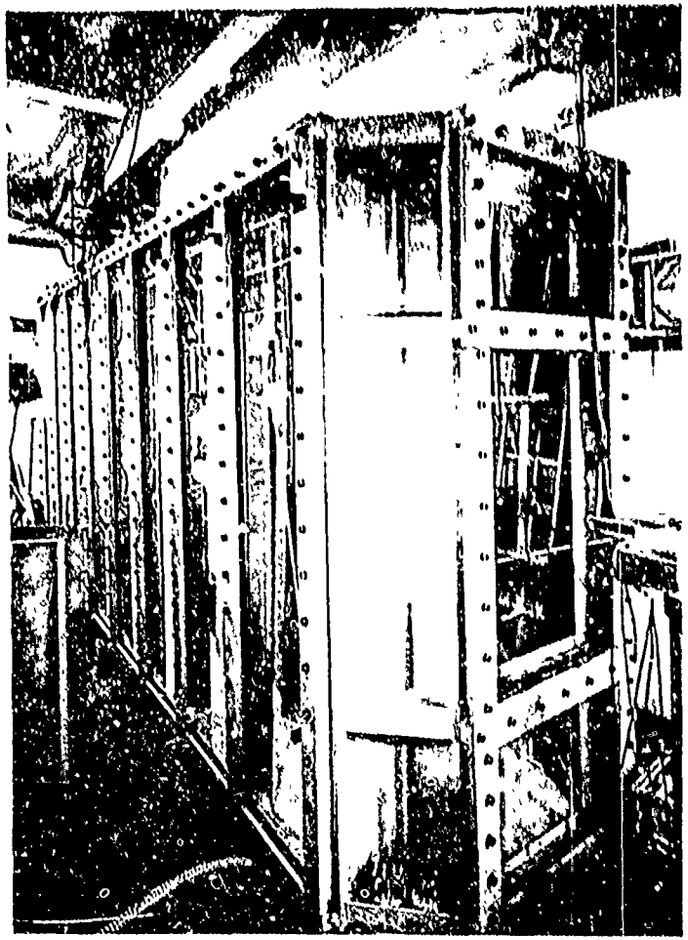

A. PHOTOGRAPH

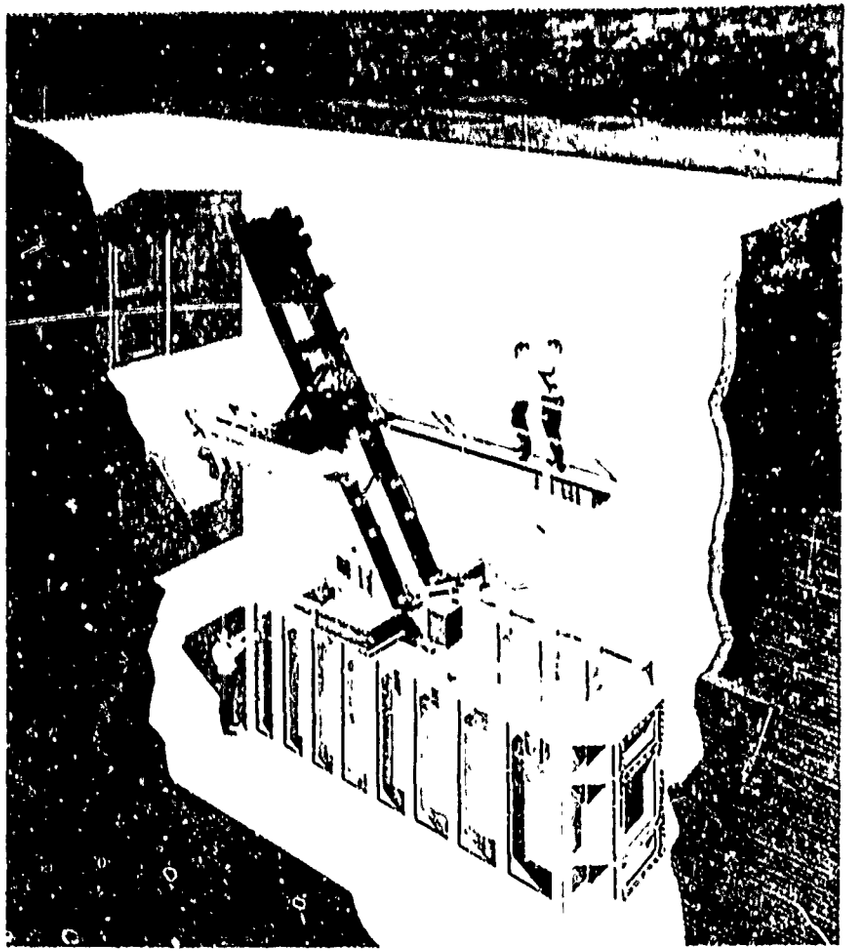

B. ARTIST'S CONCEPT

FIG. 1 HYDROBALLISTICS PILOT TANK

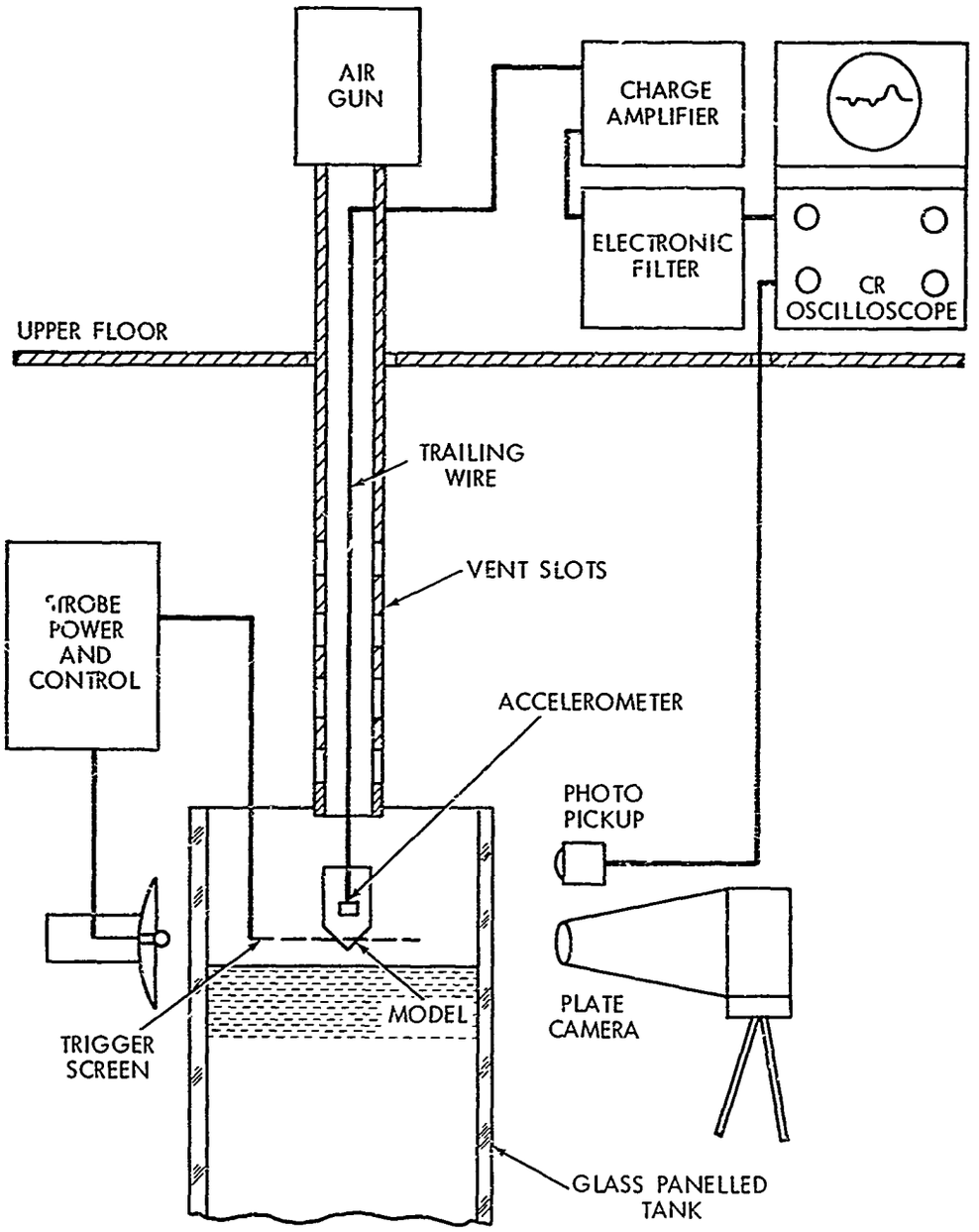

FIG. 2 TEST EQUIPMENT SCHEMATIC

the film in an open-plate camera. Located beside the camera was a photo-pickup that converted the light from the strobe into voltage that was electronically mixed with the accelerometer output in the oscilloscope. The arrangement of equipment for these tests is shown in Figure 2. The height of the trigger was adjusted such that the reflection of the model on the water surface was photographed, as well as the model. This technique resulted in two photographs, one showing the model, generally above the water surface, at three points in time; the other showing the voltage output of an accelerometer, and the time of each exposure on a common time base, displayed on an oscilloscope. Figure 3 shows a sample of these data. Additional data samples are given in Appendix A.

The models used in this test series were generally simple 3-inch base diameter cones of various half angles with cylindrical afterbodies in which the accelerometer was mounted. In some cases a sealing nut in the base of the afterbody was employed to insure a waterproof condition for the gage. The use of the seal increased the model weight by about 100 grams. Certain of the experiments involved models of different construction when high deceleration effects were desired. A special model with a 1.5-inch-diameter changeable nose, followed by a 1.5-inch-diameter cylinder and then a pair of 3-inch-diameter drag plates was used for some experiments involving slender cones. The high drag of this model after entry caused rapid deceleration so that it did not become damaged when it hit the tank bottom. This permitted multiple tests on a single model and reduced the overall cost of the program. A 20-degree aluminum nose on this model showed no damage when launched at velocities greater than 500 feet per second into less than 8 feet of water. In all, twenty different models were tested. The model details are shown in Appendix B.

Three accelerometers were used during the test series: a high-capacitance, high-impedance multiple-crystal gage; and two similar quartz gages possessing internal electronics and low output impedance. The high capacitance of the multiple-crystal gage reduced the relative error caused by changes in capacitance in the cable (trailing wire) due to acceleration and other loads.

Quartz gages were used in the lightweight models, as well as some of the lighter than normal heavy models. An electronic low-pass filter was often used with these gages to eliminate ringing of the transducer or model.

The large capacitor crystal accelerometer was used with a charge amplifier to increase the system RC time constant when a maximum acceleration of less than 30g was expected. An electronic filter was also frequently used with this gage.

The gages, scopes, filters, and charge amplifier were calibrated as a system. Several combinations were recalibrated during the test series. Three methods of calibration were used for each gage and electronics combination employed in the test

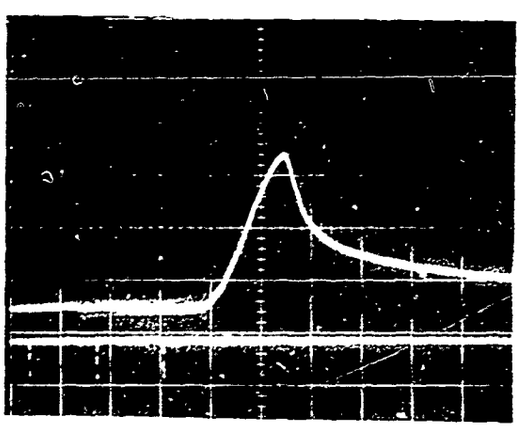

2335

series. The three calibration methods were: (1) shaker table with optical measurement of displacement; (2) shaker table with comparison with a standard gage; and (3) a one g drop.

In the one-g drop test, the gage and model were held by a short length of nichrome wire. A high current electric source was applied to the wire, causing rapid melting and quick release. This step pulse of one g was used to determine the leakage rate of the gage-electronic system, as well as to determine the gage constant.

The gage constants used for each system were the simple averages of the values determined from all of the calibration techniques.

RANGE OF VARIABLES TESTED

In the test series, a wide range of variables was investigated experimentally to establish theoretical postulations such as similitude and added mass concepts. In general, 3-inch-diameter models were tested, except for some 1.5-inch-diameter noses as explained in the previous section. This limitation in maximum diameter resulted from the maximum barrel diameter available for the air gun used. It is hoped that future tests will be conducted on much larger diameter models to investigate the conclusion reached herein that similitude does exist for cones. The ranges of test variables were as follows:

1. total cone angle - 10 to 140 degrees

2. velocity - 10.5 feet per second to 250 feet per second

3. mass - 128 grams to 9387 grams.

The distribution of these variations is given numerically in Appendix C and graphically in Figure 4.

DATA REDUCTION

The "a priori" assumptions made in the data reduction were that the external forces depend only upon size, geometry, actual velocity, and distance below the water surface; and that the law of similitude holds for cones. Additionally, it was assumed that:

1. buoyancy force is calculated from original water surface;

2. friction drag coefficient is constant for all conditions;

3. steady-state drag-coefficient is constant for each cone angle and equal to the value obtained in water-tunnel tests extrapolated to zero cavitation number (ref. 7 for 0-45 degrees, ref. 8 for 60-140 degrees, Table 1); and

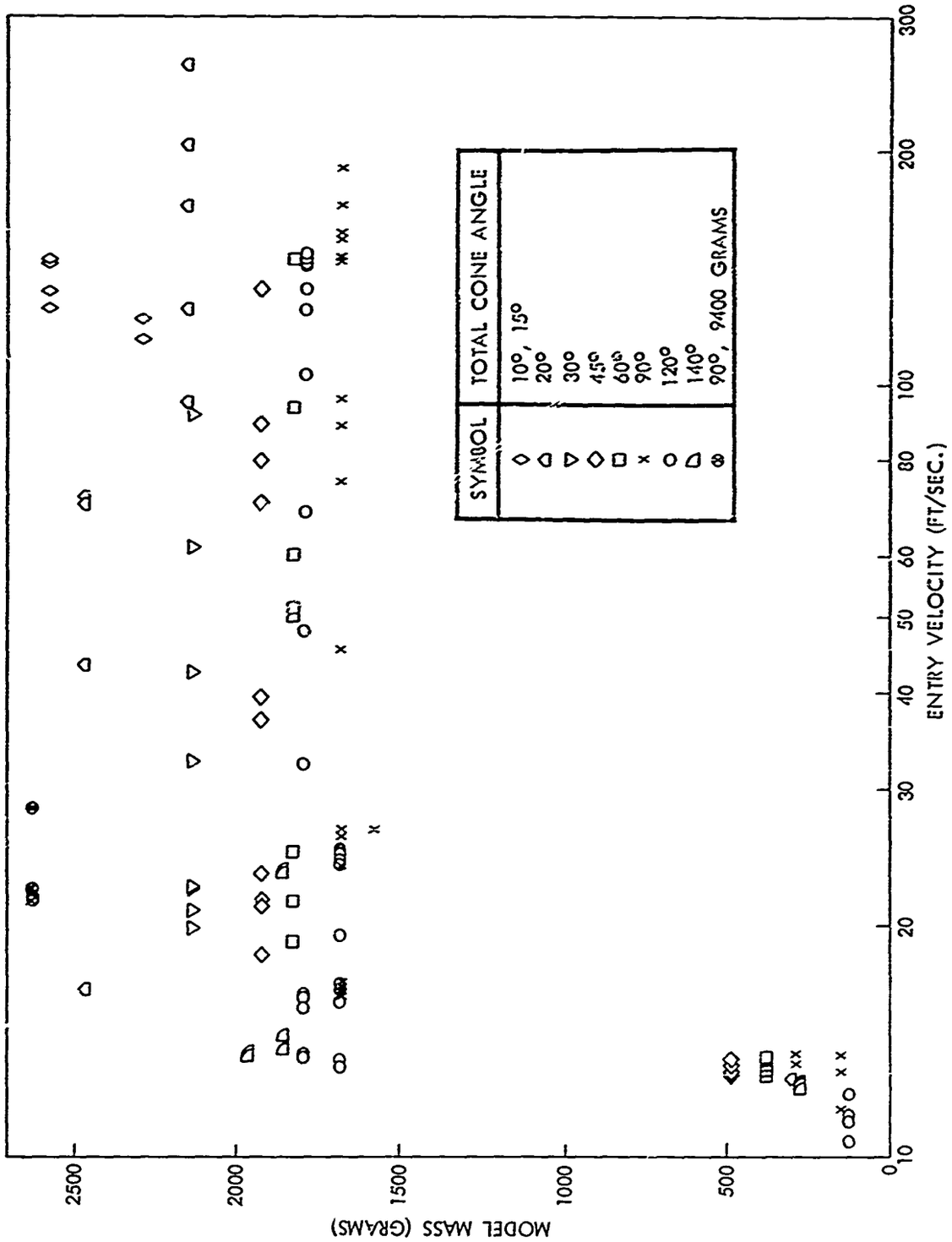

FIG. 4 DISTRIBUTION OF VARIABLES

4. surface heave-distance is proportional to the depth of penetration for each cone angle.

Table 1

Steady-State Drag Coefficient

Cone Angle	Reichardt Ref. (8)	Hoerner Ref. (7)	Value Used
10		.0595	.0595
15		.0684	.0684
20		.0866	.0866
30	.152	.1410	.141
45	.270	.257	.257
60	.365	.415	.365
90	.497		.497
120	.596		.596
140	.660		.660
180	.79		(.79)

The preliminary data reduction was done manually and involved changing the photographic records to digital form. The photographic information on the plate camera and oscilloscope records was reduced to numbers as follows: the plate camera photograph was used to determine the impact velocity and to locate the water surface relative to the oscilloscope trace. The distance the model advanced between flashes was computed using the diameter of the model as a reference dimension. The time between flashes was measured by an electronic counter and the distance from the reference picture was measured (if possible) to a point halfway between the picture and the matching reflection. Here again, the model diameter was used as the reference length.

The readings of the oscilloscope records were made using a film reader or toolmaker's microscope in the following order: the distance of a vertical cm was read to determine the scale factor; next, the pip relating the model's position with the water surface was read; and then a series of points along the trace were read. Both components of each point were recorded.

The numbers obtained from the pictures, along with recorded information such as model diameter, weight, and scope gain, were entered into a time-shared digital computer.

The acceleration time data were converted to English engineering units for computations; and when needed, a scope distoration was applied. The coordinate axis was shifted such

that zero acceleration occurred just before impact. The following correction for leakage was then applied:

$$\frac{dU}{dt}\,(\text{True}) = \frac{dU}{dt}\,(\text{read}) + \frac{1}{RC}\int_0^t \frac{dU}{dt}\,(\text{read})^{dt}$$

The coordinate axes were then shifted such that + 1g occurred just above the water and that time zero occurred at water contact. The velocity and distance were then determined for each data point using trapezoidal integration. The values related to water-entry effects were then computed.

The equation relating the momentum just before first contact with the momentum at some later time is given as Equation (1), and the force equation is given as Equation (2);

$$U_o M - U(M+m) = \int_0^t B\,dt - Mgt + \frac{\rho}{2}\int_0^t C_{ds}\,AU^2 dt \qquad (1)$$

$$-\frac{dU}{dt}\,(M+m) - U\,\frac{dm}{dt} = B - Mg + \frac{\rho}{2}\,C_{ds}\,AU^2 \qquad (2)$$

Substituting $U^2\,\frac{dm}{dS}$ for the second term of Equation (2) and rearranging terms gives:

$$-\frac{dU}{dt}\,(M+m) - B + Mg = \frac{dm}{dS}\,U^2 + \frac{\rho}{2}\,C_{ds}\,AU^2 \qquad (3)$$

If the total drag coefficient is defined as

$$C_d = \frac{2}{\rho A}\,\frac{dm}{dS} + C_{ds} \qquad (4)$$

then Equation (3) may be rewritten as

$$-\frac{dU}{dt}\,(M+m) - B + Mg = \frac{1}{2}\,\rho\,C_d\,AU^2 \qquad (5)$$

The value of added mass (m) and $\frac{dm}{dS}$ can be calculated using Equation (3) and the total drag coefficient C_d was computed from Equation (4). However, a simpler procedure is to determine m from (1) and C_d from (5). In order to ensure an accurate evaluation of the integrals in Equation (1), the added mass (m) was also computed by integrating $\frac{dm}{dS}$ as given in Equation (4) using the computed value of C_d.

For the vertical entry of cones, the added mass should be given by

$$m = \rho k R_i^{\,3} = \rho k(\tan\tfrac{\theta}{2})^3 S^3 \qquad (6)$$

Then

$$\frac{dm}{dS} = 3\rho k \left(\tan \frac{\theta}{2}\right)^3 S^2 \qquad (7)$$

Substituting (7) into (3) yields

$$-\frac{dU}{dt}(M+m) - B + Mg = \left(3\rho k\left(\tan \frac{\theta}{2}\right)^3 S^2 + \frac{\rho}{2} C_{ds} A\right)U^2 \qquad (8)$$

If the total mass constant (K) is defined as:

$$K = k + \frac{C_{ds}}{6}\left(\tan \frac{\theta}{2}\right)^{-1} \pi \qquad (9)$$

then (8) can be rewritten as

$$-\frac{dU}{dt}(M+m) - B + Mg = 3\rho K\left(\tan \frac{\theta}{2}\right)^3 S^2 U^2 \qquad (10)$$

This form of the equation was chosen to compare easily the experimental results with the theoretical results obtained in reference 3.

It should be noted that the total mass constant (K) is also a drag coefficient related to the area intersected by the original water surface. The relationship between the mass constant (K) and the total drag coefficient C_d is obtained by subtracting Equation (5) from Equation (10) and dividing out ρ and U^2:

$$C_d = 6K\left(\tan \frac{\theta}{2}\right)^3 S^2 (A)^{-1} \qquad (11)$$

If the area used to relate C_d to drag force is the area intersected by the heaved water surface, then the instantaneous drag coefficient is given by

$$C_{d_i} = \left(6K \tan \frac{\theta}{2}\right)(\pi)^{-1} \qquad (12)$$

It was expected that K, and hence C_{d_i}, would be a constant during entry, as suggested in reference 3. To investigate this, a straight line least square approximation was fitted to the computed values of K and S. The range in S extended from 20 percent to 90 percent of the depth, at which the maximum total drag coefficient (C_d) occurred. The exclusion of the first 20 percent eliminated most of the points with high relative reading errors and the last 10 percent was not used because of an observed "rolling off" as the point of separation approached.

It is seen from Equation (10) that the slope of the mass constant (K) versus depth (S) curve can be altered by changing the value of the depth (S) associated with each data point. Variations changes in S can be accomplished by adjusting the value of the distance to the water obtained from the plate camera

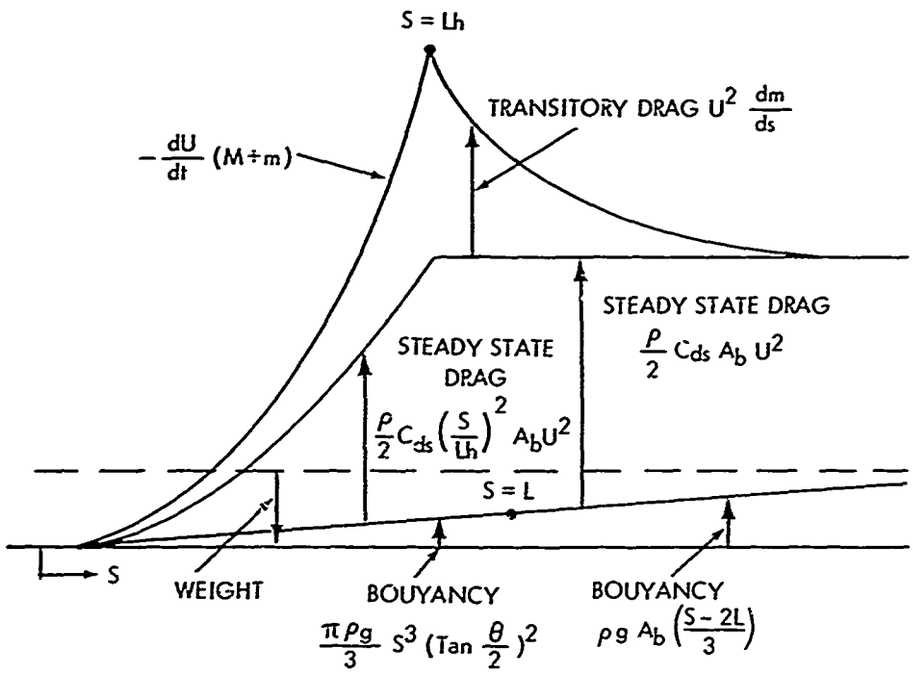

FIG. 5 FORCE MODEL VS DEPTH

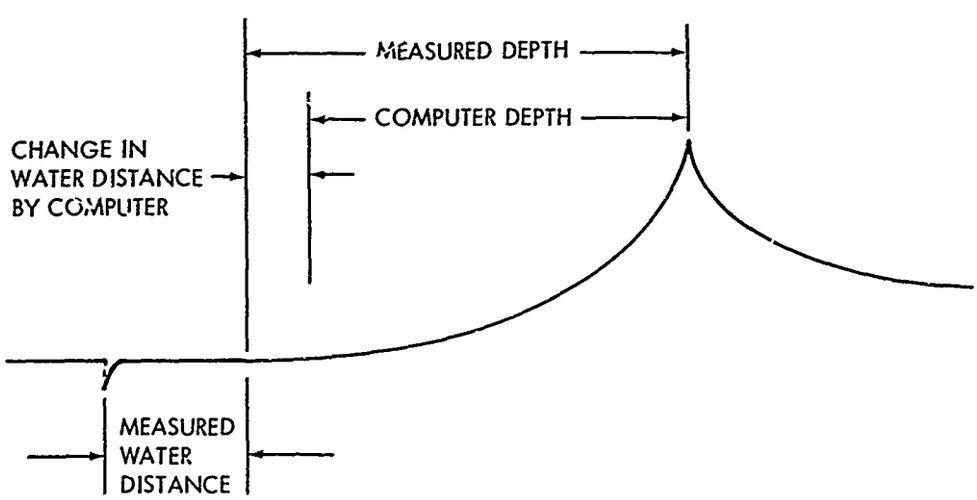

FIG. 6 MEASURED DEPTH COMPARED TO COMPUTER DEPTH

film. This value was systematically changed by the computer until a movement of .0005 of the cone length would cause a sign reversal in slope. This slope was then recorded, as was the sum of the squares of the residuals between the least square fit and the data points.

The computed depth was that at which the maximum total drag coefficient occurred after the least square perturbations. A measured depth was obtained for many tests either by comparing the distance to the water measured from the film, with the value arrived at by the computer, as shown in Figure 6; or, in a few cases, directly from the photograph and scope trace.

The penetration ratio h was computed by dividing the computed depth by the cone length. A related term is the surface heave defined as the cone length minus the computed depth. The numerical results for each test are given in Appendix C.

RESULTS AND CONCLUSIONS

Perhaps the most important result of the entire test series is proof that the total added mass constant K is indeed constant as the cone is wetted. A constant K implies from Equation (12) a constant instantaneous drag coefficient C_{d_i}, and from Equation (9) a constant added mass constant (m). After the perturbation in distance, the average measured point was within 3.6 percent (root mean square) of a constant value. Also, a comparison of all measured depth and corresponding computer depths shows an average difference of .54 percent. To the satisfaction of the author, these results show that K, m and C_{d_i} are constants over the range of depths used in the least square fit. There seems to be a skew of about .3 percent between computed depth and measured depth, as shown in Table 2.

Table 2

Comparison of Measured Depth and Computer Depth

Rank	Cone Angle	Shot No.	Difference (inches/inch)	Aggregate Error %
0	-	-	-	.54
1	30	1895	.1467	.28
2	45	1662	.1295	.58
3	20	1902	-.0927	.23
4	90	1695	-.0844	.40
5	120	1997	.0822	.25
6	30	1888	-.0754	.40
7	140	2024	-.0735	.56

Table 2 (Cont.)

Rank	Cone Angle	Shot No.	Difference (inch)	Aggregate Error
8	140	201405	.0714	.43
9-14	-	6 pts	.06-.07	-.11
15-22	-	8 pts	.05-.06	+.49

The table shows the effect of discarding data points in descending order of percent difference. Perhaps this difference is due to a systematic reading error.

It is hoped that one of the major contributions of this report is the determination of total drag coefficient (C_d) for most cone angles. To be of maximum utility, C_d should be independent with respect to velocity, size, and weight. In order to investigate the velocity dependence, all reported values of C_d (Appendix C) were normalized and a least square fit to $C_d = A+BU_o$ performed. This calculation resulted in $C_d = 1.008 - .00012U_o$. The results should be useful in sizes below and above those tested because of similitude. The author could see no systematic effect on C_d due to varying weights. As seen in Table 3, the drag coefficient for the 90-degree, 3-inch-diameter cones remained within 2 percent of the average for a model weight range from .33 pound to 20.9 pounds.

Table 3

Maximum Drag Coefficients for Various Model Weights

Cone Angle	Normal Weight	Odd Weight	Odd Wt C_d / Av Wt C_d
140	1900 (6)	251 (3)	.971
120	1700 (26)	128 (4)	.954
		287 (2)	.949
90	1600 (17)	150 (3)	.992
		284 (2)	1.011
		9489 (4)	1.018
60	1800 (8)	(5)	.985
45	1900 (10)	(4)	1.057
20	2200 (9)	295 (1)	.935

No odd weights were tested at cone angles of 30, 15, or 10 degrees.

The blunt cones (120 degrees and 140 degrees) did indeed show a reduction of about 5 percent for the light models. This is believed to be due to errors in the gage constant (large percent slowdown), model weight (how much wire to include), and trace reading errors. The average maximum total drag coefficient for each cone angle as a function of this angle is shown in Figure 7. Also shown in Figure 7 are values derived from reference 5 and those assumed for C_{ds}, Table 1. Note the basic agreement of values of maximum drag coefficient and the convergence of C_d to C_{ds} for the smaller cone angles. The curve shows that the total drag coefficient is approximately equal to the steady-state drag coefficient from zero cone angle to a total cone angle of about 45 degrees, above which rapid divergence occurs. Another way of stating this is that the maximum shock factor during impact as a function of cone angle is almost unity up to 45 degrees, and then rapidly increases to values of 2 and 5 for blunter cones. Also, note the excellent agreement with the theoretical values (Wagner and Schneider, reference 5) and the general agreement with the experiments of Mager and Watanabe (reference 4).

An important result of these tests is the percent of the cone submerged (based upon original water surface) when the maximum total drag coefficient occurs. These data are shown in Figure 8. Again, reasonable agreement occurs when compared with previously selected tests.

It is seen that if the cone angle is very small, then the maximum drag coefficient occurs after the cone base passes the original water surface. The number of tests conducted on 10-degree and 15-degree total angle cones leaves this point somewhat in doubt. For blunter cones, the percent of cone length penetrated drops as the cone angle increases until a value of 71.5 is reached for 140-degree cones. This is equivalent to 51.1 percent of area below the original water surface. When compared to the simple theory used in reference 2, this change in radius could change the added mass by almost three to one.

Comparison of the test results with theory is best shown in Figure 9, where the experimental values of total mass constant (K) are corrected for friction and compared with the theoretical values arrived at in reference 3. Also plotted in Figure 9 are experimental values obtained from reference 3. For small total cone angles, the theoretical values are much greater than those obtained from the experiments even with the steady-state drag term added to the added mass. For very blunt cones, the theoretical predictions seem to be too small. The values of added mass constant derived in reference 3 from the tests described in reference 4 are monotonic, decreasing with respect to increasing depth. These could probably be brought into agreement with the law of similitude by a slight change in time of impact.

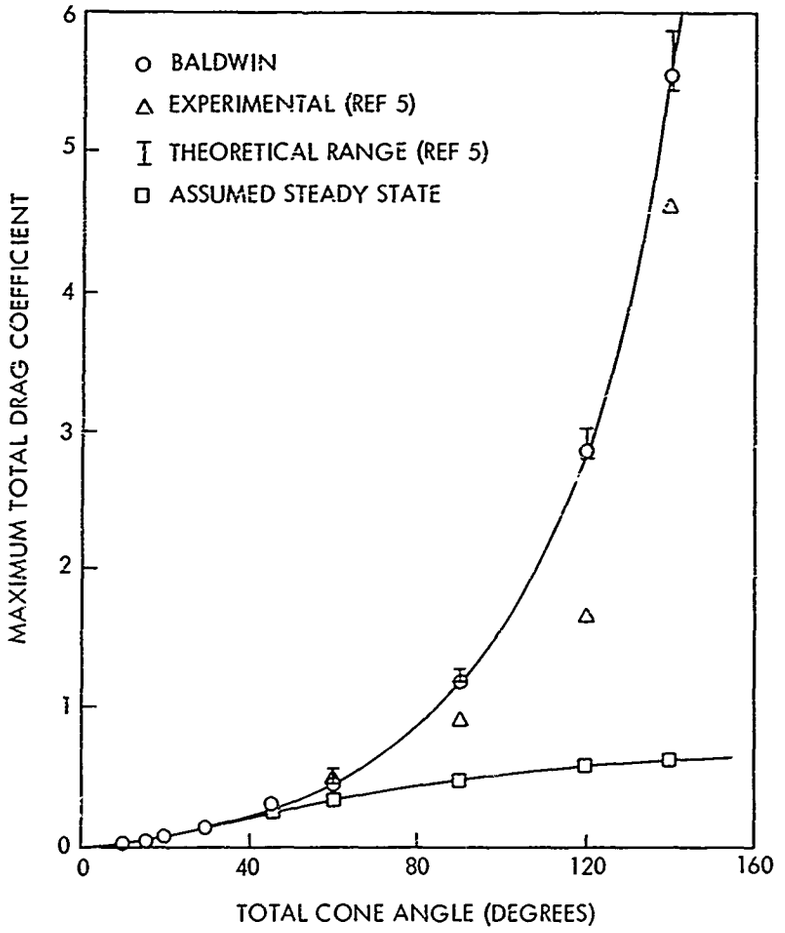

FIG. 7 MAXIMUM TOTAL DRAG COEFFICIENT VS TOTAL CONE ANGLE

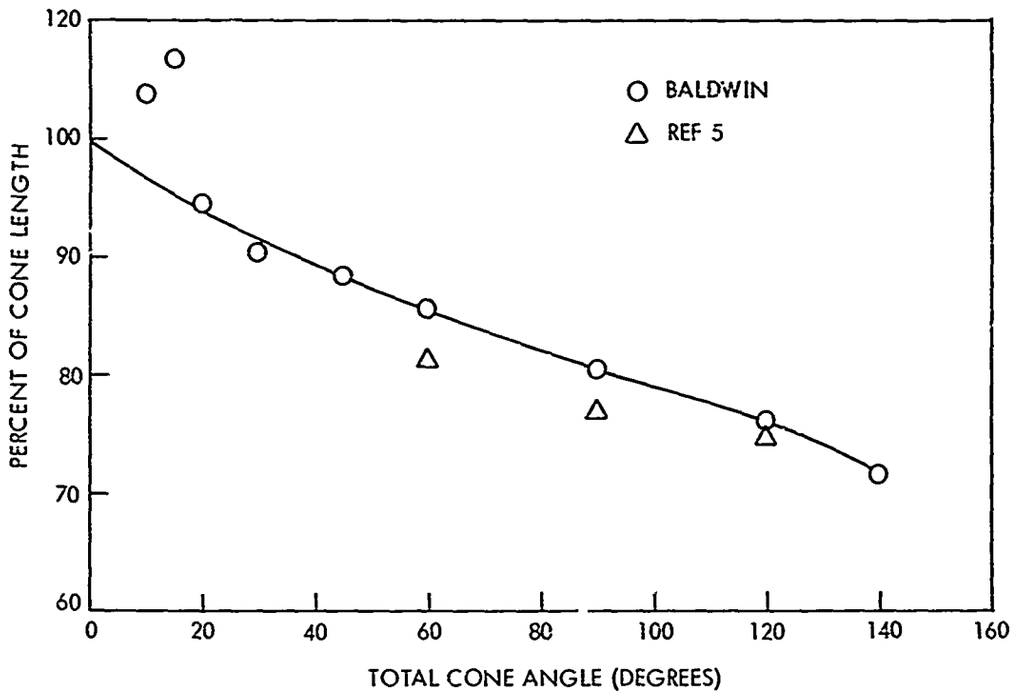

FIG. 8 PENETRATION RATIO VS TOTAL CONE ANGLE

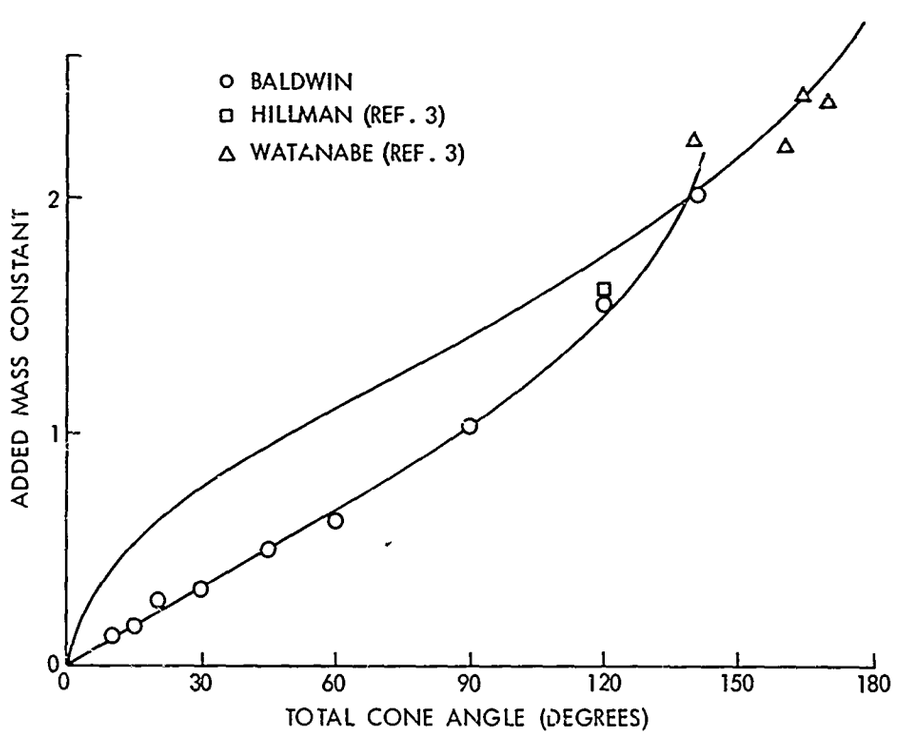

FIG. 9 TOTAL ADDED MASS CONSTANT VS TOTAL CONE ANGLE

The uncorrected mass constants versus cone angle for fine cones are shown in Figure 10 as is the effect of assuming a friction drag coefficient (C_f) of .0031. It is seen that the subtraction of skin friction causes the curve of the mass constant to pass through zero for zero cone angle. The friction effect was also used to correct the total drag coefficient C_d, see Figure 7.

In general, for each cone angle, C_d, k, K, and m did not seem to vary with velocity or mass of the model over the range of variables tested.

Another important result is the amount of added mass accumulated during entry. The experimental values of added mass (m) associated with maximum drag coefficient versus cone angle are shown in Figure 11. As shown in Figure 5, the final results regarding added mass are strongly dependent on the assumptions made concerning C_{ds}. Changes in these assumptions, if desired in the future, may be made analytically as seen from Figure 5. Note that the added mass constant (k) will not give the same exact values of m due to the roll-off experienced as the point of maximum total drag coefficient is approached. The added mass constants defined by the equations:

$$m = \rho k S^3 \tag{13}$$

and

$$m = \rho k \left(\frac{S}{h}\right)^3 \tag{14}$$

are shown versus total cone angle in Figure 12. The average added mass associated with the maximum total drag coefficient, the cone length, and the average penetration ratio were used to compute each plotted point.

As a body enters the water, the amount of added mass should increase after the maximum drag coefficient is experienced due to water surface effects. This is shown graphically in Figure 5. The values of added mass for points near and after $C_{d_{max}}$ for many tests are given in Appendix C. The added mass is shown over the entire range of depth for three tests in Figure 13. These results are in qualitative agreement with reference 9. For many of the tests with slender cones, the added mass curve did not become level at as great a depth as those shown on Figure 13, Appendix C. It is believed that this premature reduction in added mass was caused by using unstable models that developed significant angles of yaw after entry and thus misaligned the accelerometer axis with respect to the velocity vector.

The photographs taken by the plate camera sometimes contained an image of the model entering the water in addition to the required above-water information. A study of these splash pictures and associated acceleration traces leads to the conclusion that the maximum deceleration occurs as soon as the base area

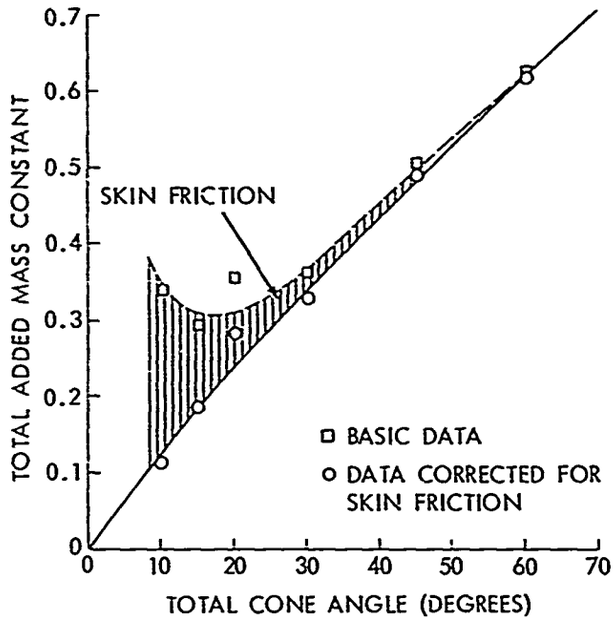

FIG. 10 CORRECTION OF TOTAL ADDED MASS CONSTANT VS TOTAL CONE ANGLE

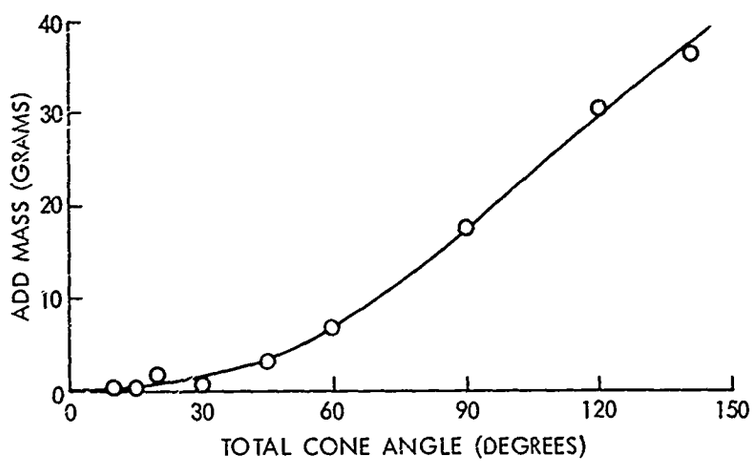

FIG. 11 ADDED MASS ASSOCIATED WITH MAXIMUM DRAG COEFFICIENT VS CONE ANGLE

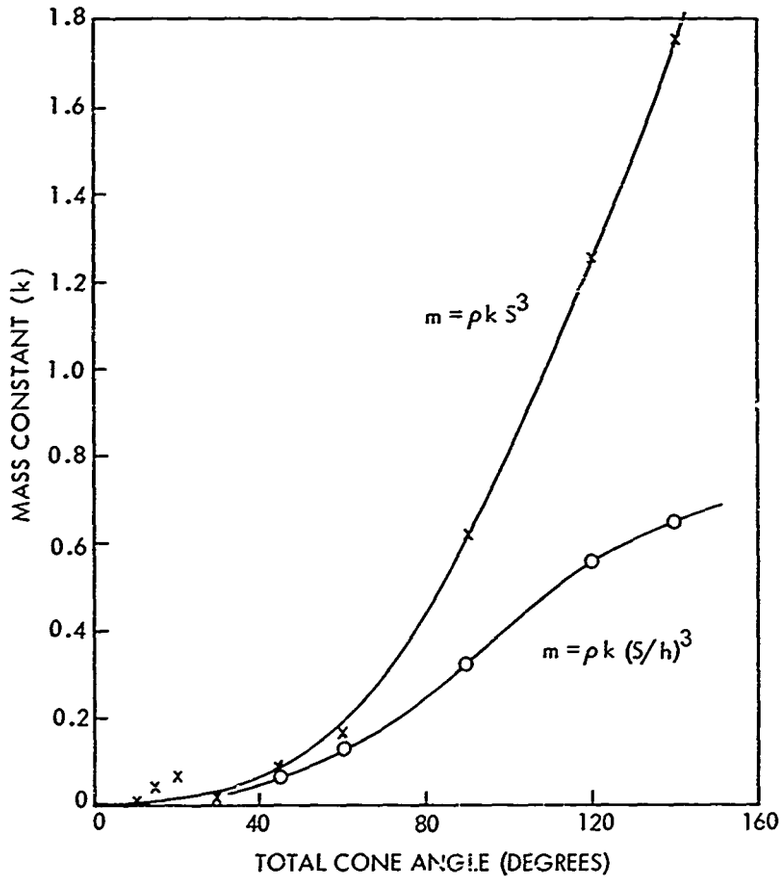

FIG. 12 ADDED MASS CONSTANT VS TOTAL CONE ANGLE

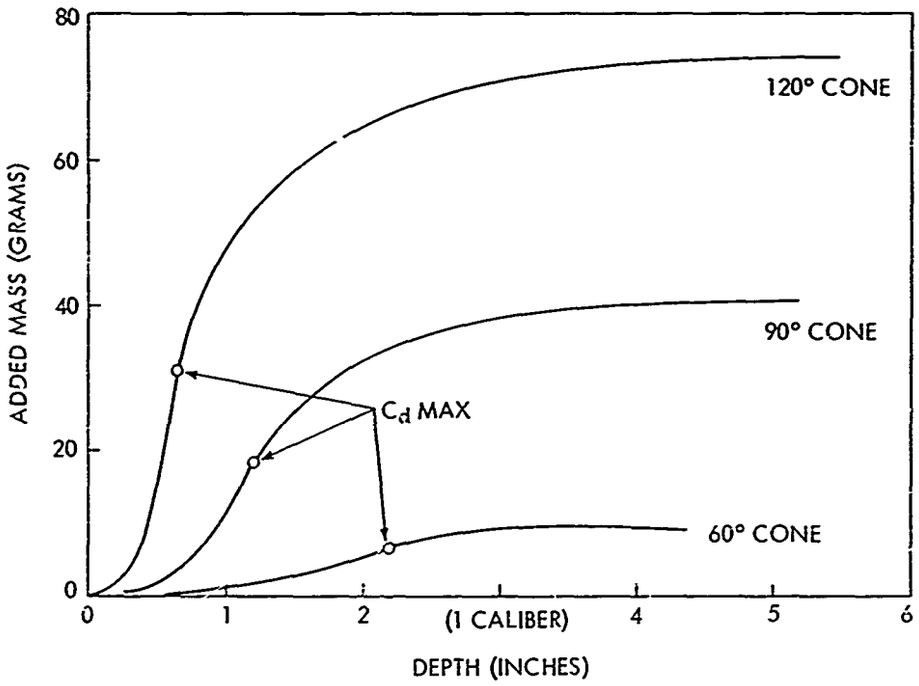

FIG. 13 ADDED MASS VS DEPTH

bears upon solid water for the blunter cones and somewhat later for the slender cones. The data from shots 1847 and 1687 included in Appendix A were among those used to reach this conclusion.

APPLICATION OF RESULTS

The practical application of these results will yield the prediction of the axial forces experienced by conical bodies during vertical water entry. In computing these forces, Equation (15) may be used:

$$-\frac{dU}{dt}(M+m) - B + Mg = \frac{1}{2}\rho Cd(S)A_b U^2 \qquad (15)$$

or in another form:

$$-\frac{dU}{dS}(M+m) - \frac{B-Mg}{U} = \frac{1}{2}\rho C_d(S)A_b U \qquad (16)$$

Note that the internal body forces and equal external pressure forces (axial) are given by:

$$Mg + \int P\, dA = F = M\frac{dU}{dt} \qquad (17)$$

For any particular design known constants include: total cone angle (θ), missile mass (M), base radius (R), and initial velocity (U_o). In Equation (16), the remaining functions are: added mass (m), buoyancy (B) and total drag coefficient ($C_d(S)$). Due to the shape of these functions, it is necessary to determine their values over two ranges of depths. From contact until the depth at which the total drag coefficient is obtained. The functions for added mass m and total drag coefficient are given by

$$m = \rho k S^3 \qquad (18)$$

$$C_d(S) = (C_{d_{max}}(\frac{S}{Lh})^2) \qquad (19)$$

For depths greater than Lh, these functions are given by

$$m = \rho k(Lh)^3 + \int_{Lh}^{S} \frac{\rho A_b}{2}(C_{ds} - C_{ds})ds \qquad (20)$$

$$C_d(S) = ((C_{d_{max}}) - C_{ds})\ \frac{A}{1.3} + C_{ds} \qquad (21)$$

where

$$A = \exp[-\frac{9(.661)(S-Lh)}{Lh}] + .3\div[1 + (\frac{S-Lh}{R})]^2 \qquad (22)$$

$C_d(S)$ in this case is a curve fit to the data. The values of $C_{d_{max}}$ and C_{ds} used in Equations (19), (20), and (21) should include

the effect of skin friction. For example, if the Reynolds number is about 6×10^6, then .003 cotan $\frac{\theta}{2}$ should be added to the values obtained from Figure 7.

The values of k used in Equations (18) and (20) are obtained from the upper curve of Figure 12.

From contact until the cone base is level with the original water surface the buoyancy is given by

$$B = \frac{\rho g \pi}{3} (\tan \frac{\theta}{2})^2 S^3 \tag{23}$$

and for greater depths (S>L)

$$B = \rho g \pi R^2 (S - \frac{2}{3} L) \tag{24}$$

Note these equations neglect "roll off", which should give negligible errors. If greater accuracy is desired, use m derived from K up to 80 percent immersion, and a smooth function to the peak value. The only remaining unknowns in Equation (16) are U and $\frac{dU}{dS}$ which can be solved for by various numerical methods. One of the simplest assumes that the velocity U is U_o for the first try, and U (from a preceding try) for each succeeding iteration. When U is determined, then the acceleration $\frac{dU}{dt}$ may be solved for directly using Equation (5). A simple computer program for solving this problem is given in Appendix D. Example runs for a 3-inch, 5-pound, 90-degree cone and an 18-inch, 18-pound, 90-degree cone are also included. The relatively large decelerations of the large light cone caused the maximum deceleration to occur before the maximum total drag coefficient.

RECOMMENDATIONS

Based upon the experience gained from this test series and the results thereof, the author recommends in addition to confirming tests, that the following work be conducted regarding vertical water entry of cones:

1. Axial forces experienced by cones during water entry be extended to significantly higher velocities.

2. Assumptions of buoyancy and C_{ds} be confirmed: buoyancy, by very large models; and C_{ds}, by a method suggested in reference 10, by testing two geometrically similar models of differing mass, and solving simultaneously for C_{ds} and m using Equation (3).

3. Effects of angle of attack at entry be determined.

4. Investigation as to why the added mass maximizes before complete cavity development be made.

REFERENCES

1. W. E. Parr, "The Water Entry Problem with Bibliography," NOLTR 66-173, 1966

2. W. R. Hoover and P. J. Reardon, "Approximate Impact of Drag Coefficients for the Vertical Water-Entry of Families of Cone, Ellipsoidal, and Tangent Ogive Nosed Missiles," NOLTR 64-110, 1964

3. M. Schiffman and D. C. Spencer, "The Force of Impact on a Cone Striking a Water Surface (Vertical Entry)," Comm. Pure and Appl. Math., Vol IV (1951)

4. S. Watanabe, "Resistance of Impact on Water Surface," Inst. Phys. Chem. Res., Tokyo (Sci Papers), 1930-1934

5. A. Weible, "The Penetration Resistance of Bodies with Various Head Forms at Perpendicular Impact on Water," German Avia Res. Report No. 4541, Naval Research Laboratory Transl. NRL trans. No. 286, revised (1952)

6. G. Mosteller, "Axial Deceleration of Bodies at Oblique Water-Entry of 2-inch Diameter Models with Hemisphere and Disk-Cylinder Noses," NAVORD Report 5420, 1957

7. S. F. Hoerner, Fluid Dynamics Drag, pp. 20-24, 1965

8. H. Reichardt, "The Laws of Cavitation Bubbles at Axially Symmetric Bodies in a Flow," Ministry of Supply Transl. GDC No. 10/5678T, 1945

9. J. G. Waugh and A. T. Ellis, "Fluid-Free-Surface Proximity Effect on a Sphere Vertically Accelerated from Rest," Hydronautics Vol 3 No. 4, Oct, 1969

10. V. C. D. Dawson and A. E. Seigel, "The State of the Art of Water-Entry Technology," NOLTR 70-209 of 14 Sep 1970

APPENDIX A

The original data from several tests form this appendix. These particular tests were selected to provide information at most cone angles for both heavy and light models. Shot numbers, weight, gage constants and other necessary numeric values are given in Table A-1. The remainder of this appendix contains optical copies of the original data photographs.

Table A-1. Numerical Constants

Shot no.	Cone angle (deg)	Weight (gm)	Gage constant (ft/sec²/V)	Time constant (sec)	Scope gain (V/cm)	Scope sweep (msec/cm)	Time between pictures (msec)	Remarks
1904	20	2459	50.9	.08	1-2	5.0	4.04	model still in barrel when trace begins. 1.. cone diameter. Note muzzle blast
1916	20	538	152.7	.08	5.0	0.5	1.0	
1893	30	2136	152.7	.08	.2-.5	5.0	5.00	picture near max acceleration
1675	45	1922	152.7	.08	1-.5	2.0	2.00	
2337	45	482	3206	.3	.02	5.0	6.69	
1687	60	1829	50.9	.08	2-.5	5.0	5.05	picture near max acceleration
2429	60	379	2966	.08	.02	5.0	6.67	
1654	90	1676	2219	.018	5.0	1.0	1.0	
2431	90	284	3204	.3	.05	10.0	6.68	
2435	90	150	3204	.3	.05	5.0	6.68	Figure 3
2449	90	9387	2927	.08	.01	5.0	4.00	
1981	120	1789	2332	.018	1.0	2.0	2.0	
2032	120	1678	3138	.75	.02	5.0	6.66	
2061	120	128	3138	.75	.1	5.0	10.03	large amount of roll-off
21404	120	287	2808	.08	.2	5.0	10.0	small amount of roll-off
2023	140	251	3138	.75	.2	5.0	5.0	small amount of roll-off
2026	140	1810	3138	.75	.05	5.0	6.67	

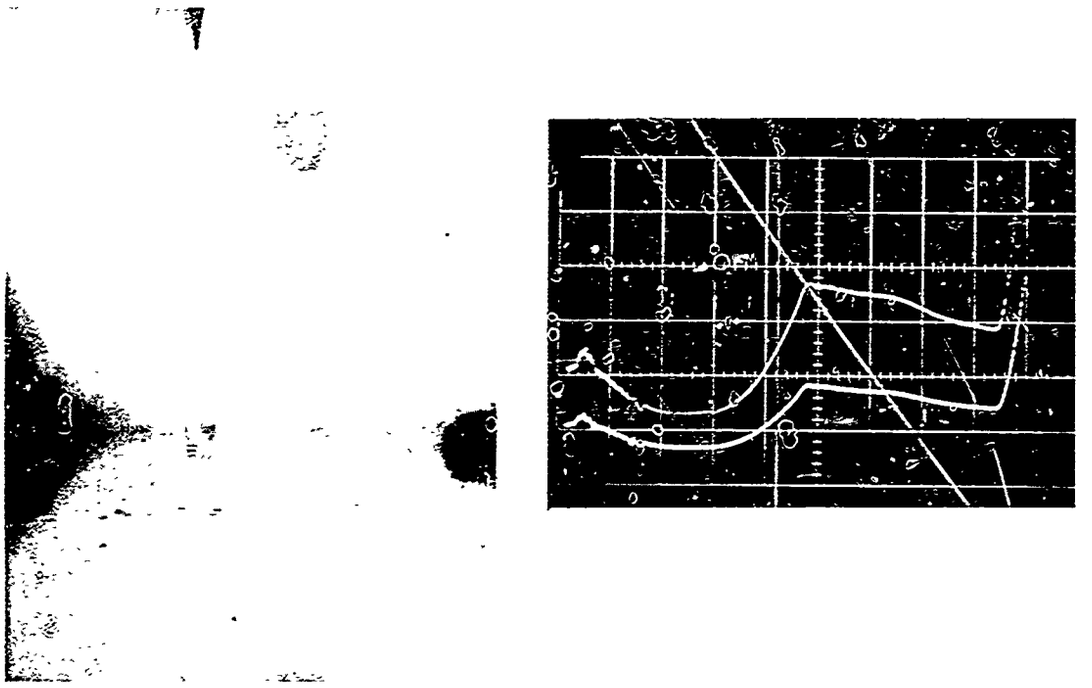

1904

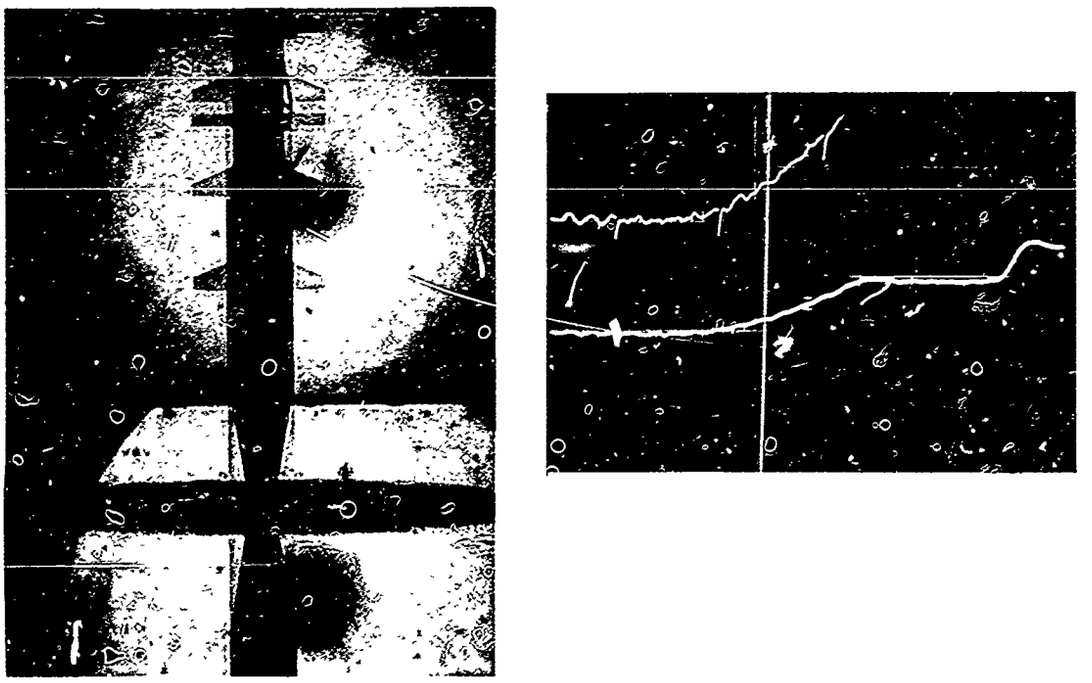

1916

FIG. A-1 ORIGINAL DATA - SHOTS 1904, 1916

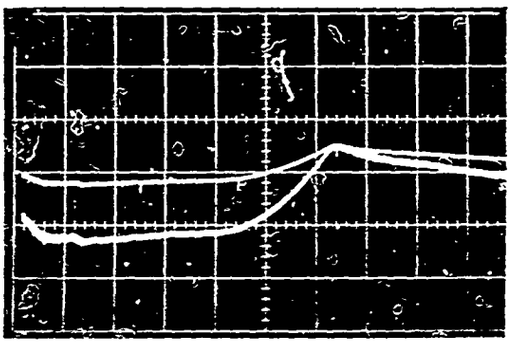

1893

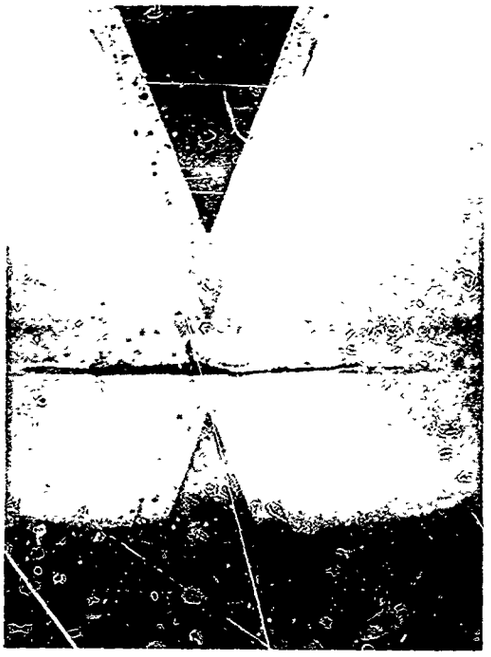

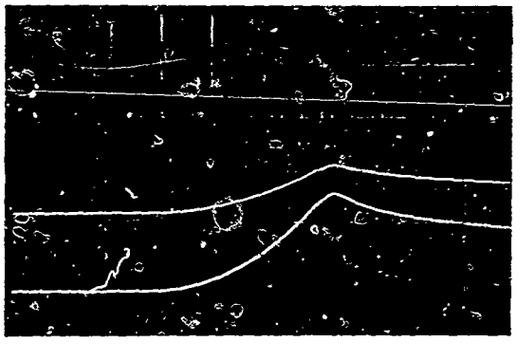

1675

FIG. 4-2 ORBITAL DATA - [illegible]

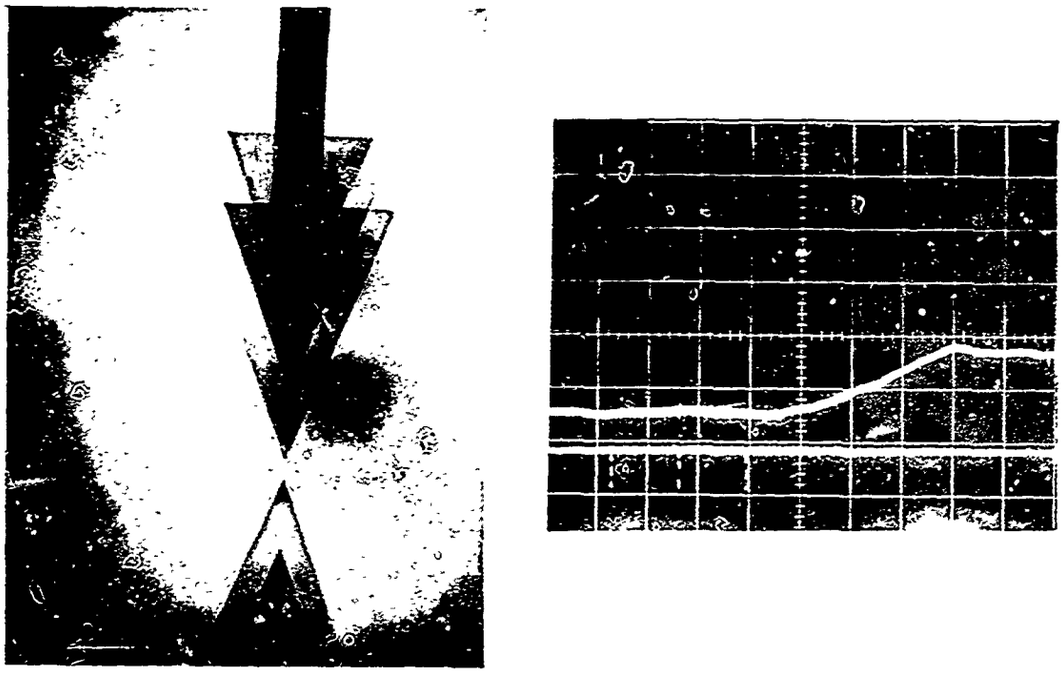

2337

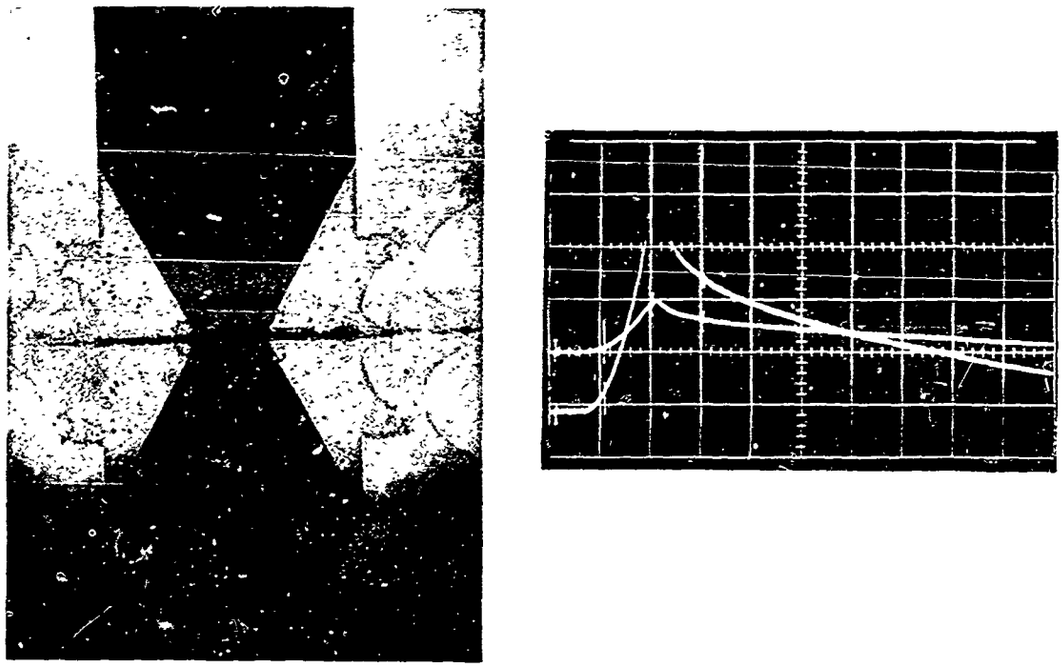

1687

[illegible] A-3 ORIGINAL DATA - [illegible]

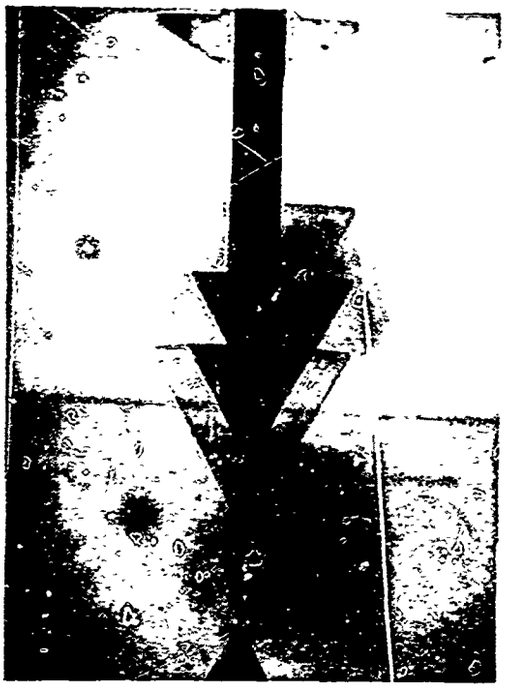

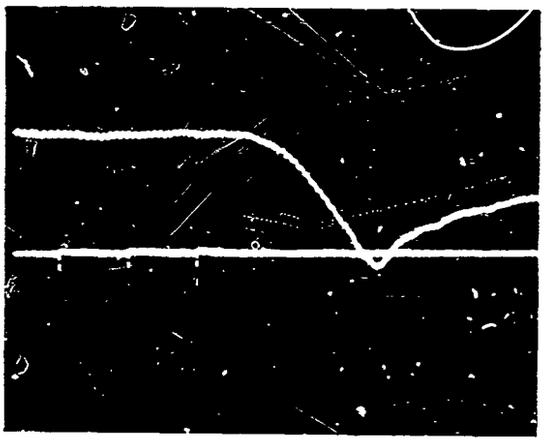

2429

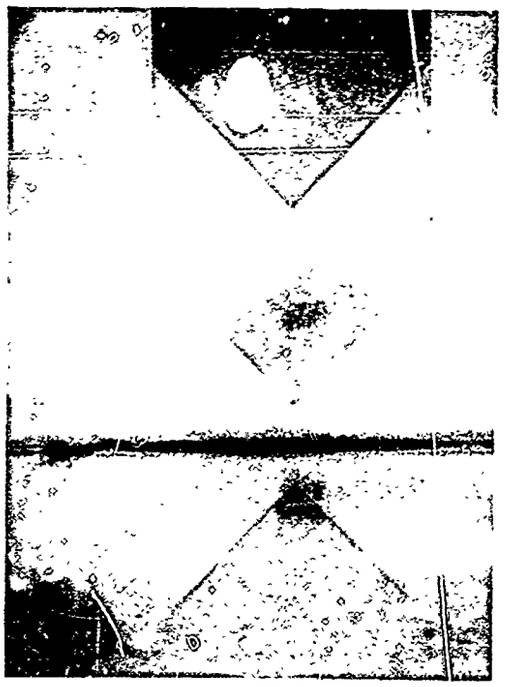

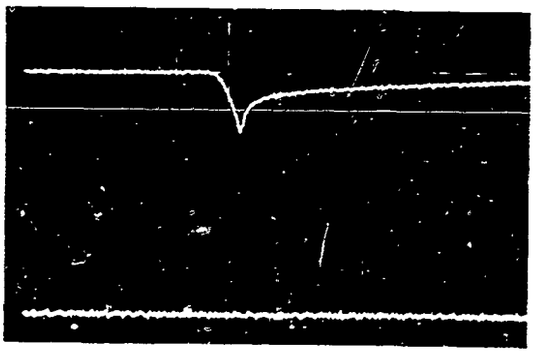

1654

FIG. A-4 ORIGINAL DATA - SHOTS 2429, 1654

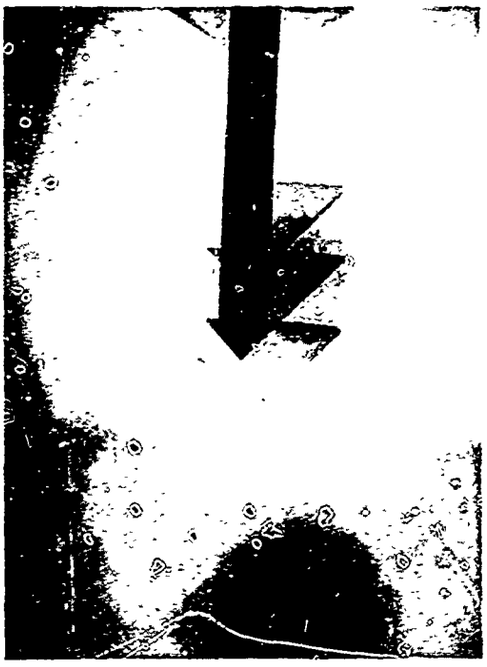

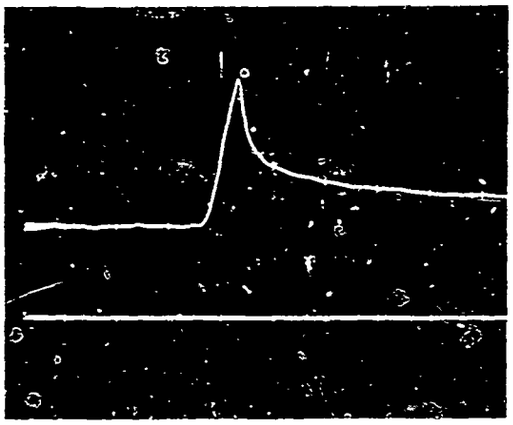

2431

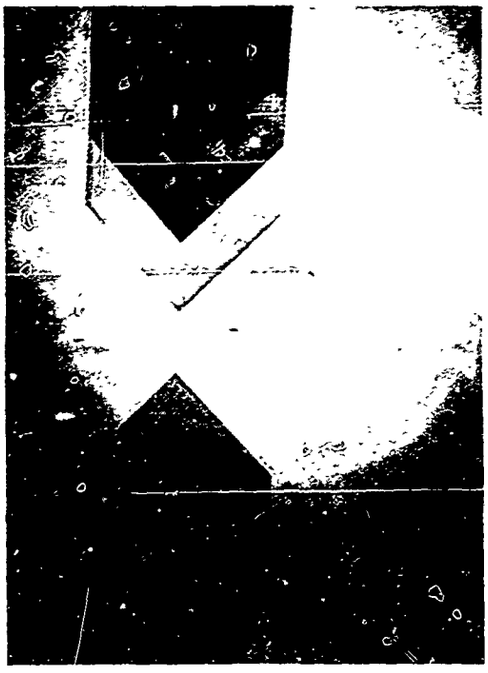

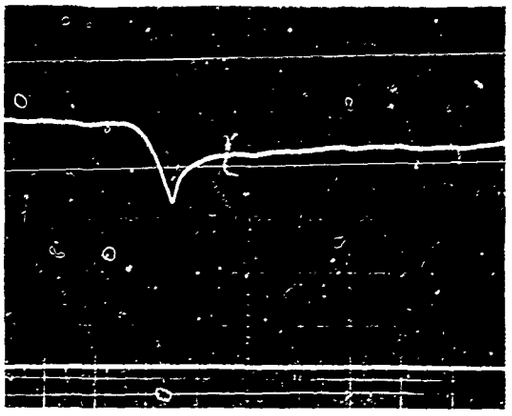

2449

FIG. A- EXPERIMENTAL DATA -

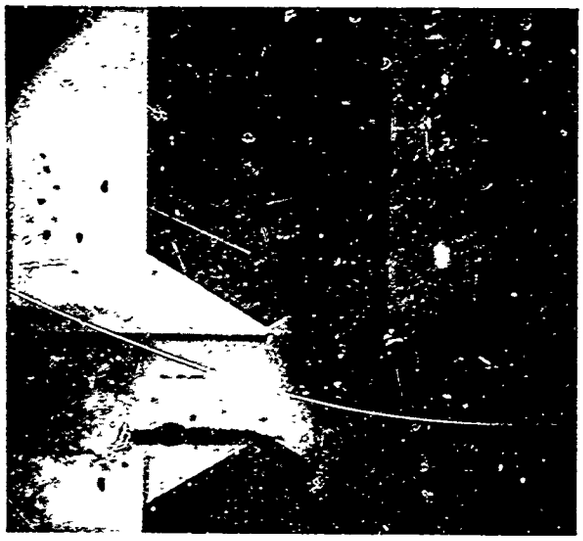

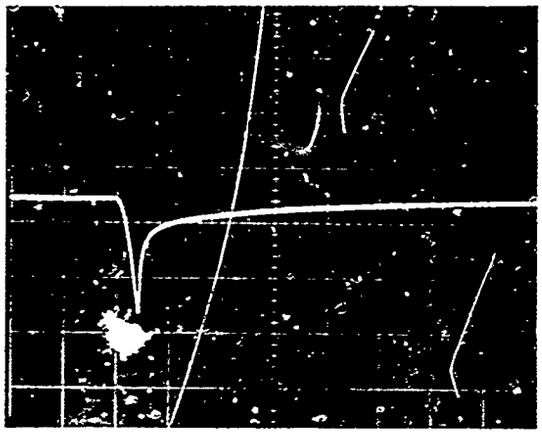

1981

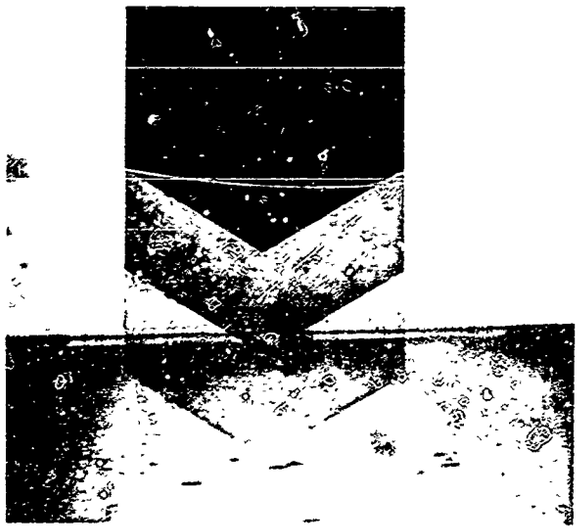

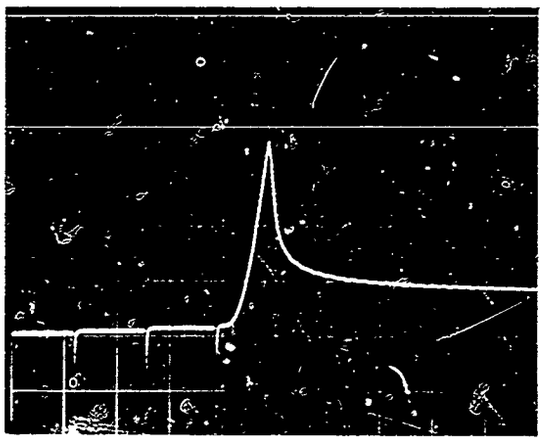

2032

[illegible] - [illegible] DATA - [illegible]ES [illegible]

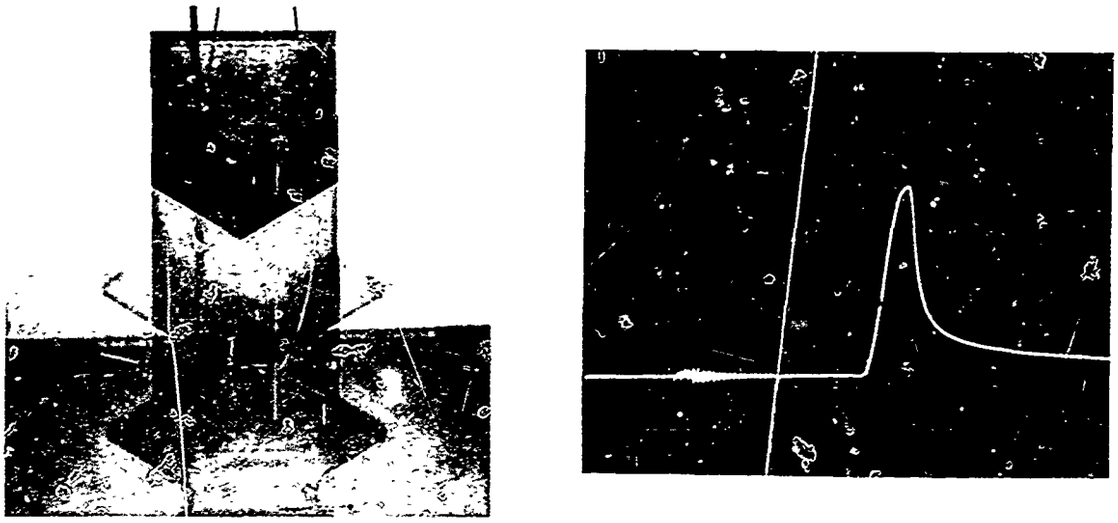

2061

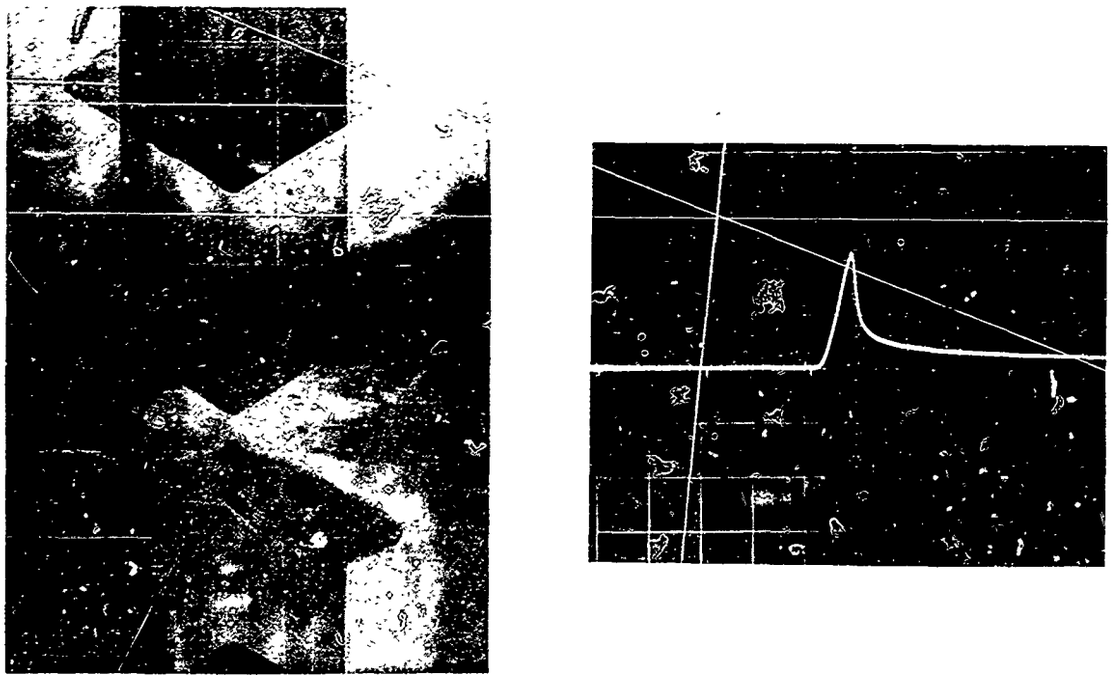

21404

FIG. A-7 ORIGINAL DATA - SHOTS 2

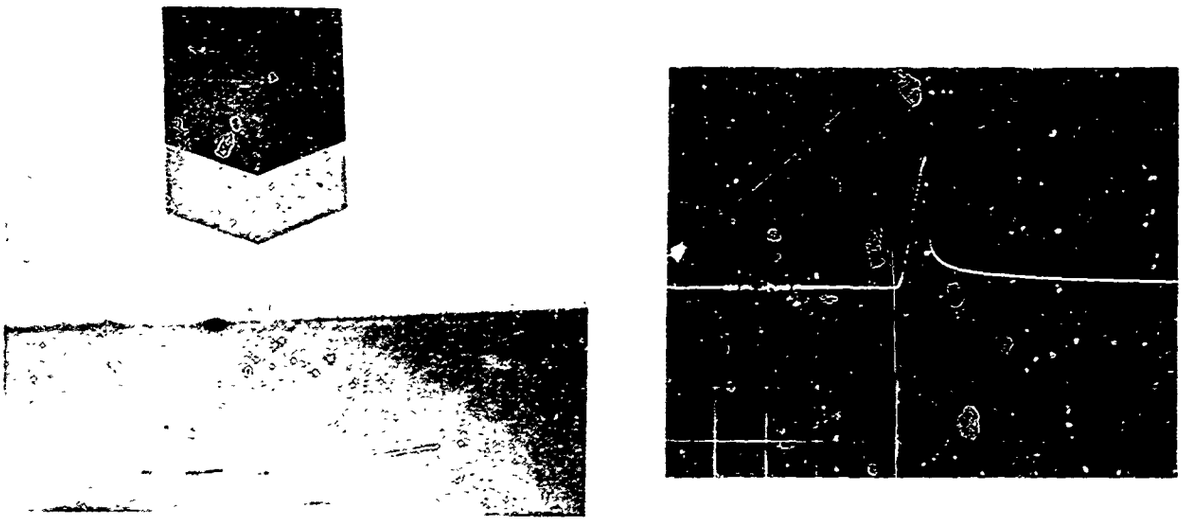

2023

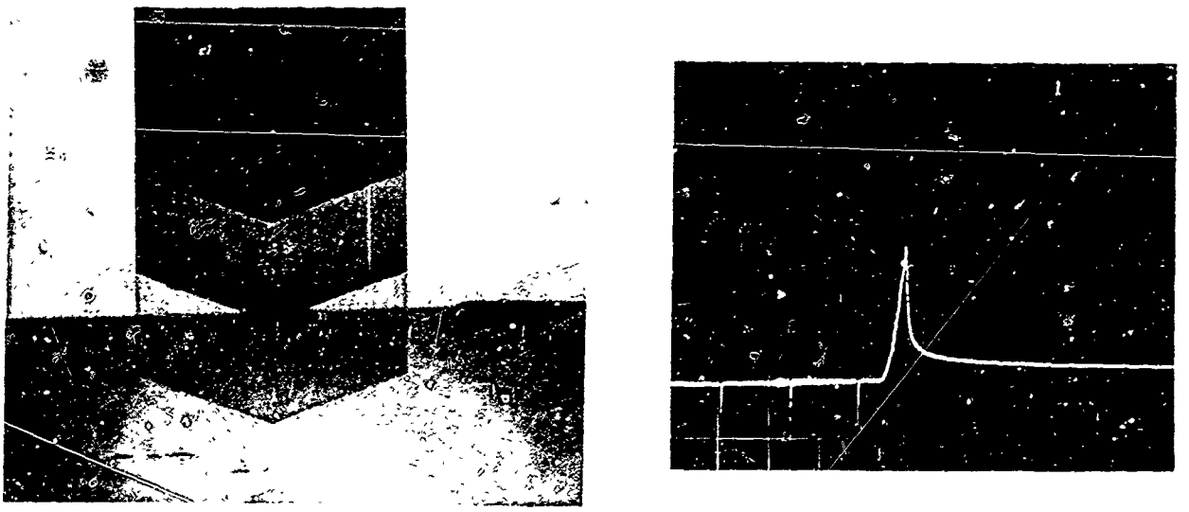

2026

FIG. A-8 ORIGINAL DATA - SHOTS 2023, 2026

APPENDIX B

This section consists of sketches depicting the various models tested during this series. The measured variation from the nominal values used to reduce the data were:

3-inch base diameter + .000 - .003 inch
1.5-inch base diameter ± .001 inch
Cone angle ± .1 degree for cone angles of 10 through 30 degrees and 140 degrees
± .3 degree for cone angles of 45 through 120 degrees

As the test series progressed, a slight rounding of some cone tips occurred, due to repeated hitting of the nylon impact mats used to stop the models. The maximum tip radius was measured as .035 inch. As mentioned before, the use of the drag plate model (Figure B-2) eliminated noticeable tip damage for aluminum cones as fine as 10-degree total angle. No correction was attempted for the rounding of the cone tips.

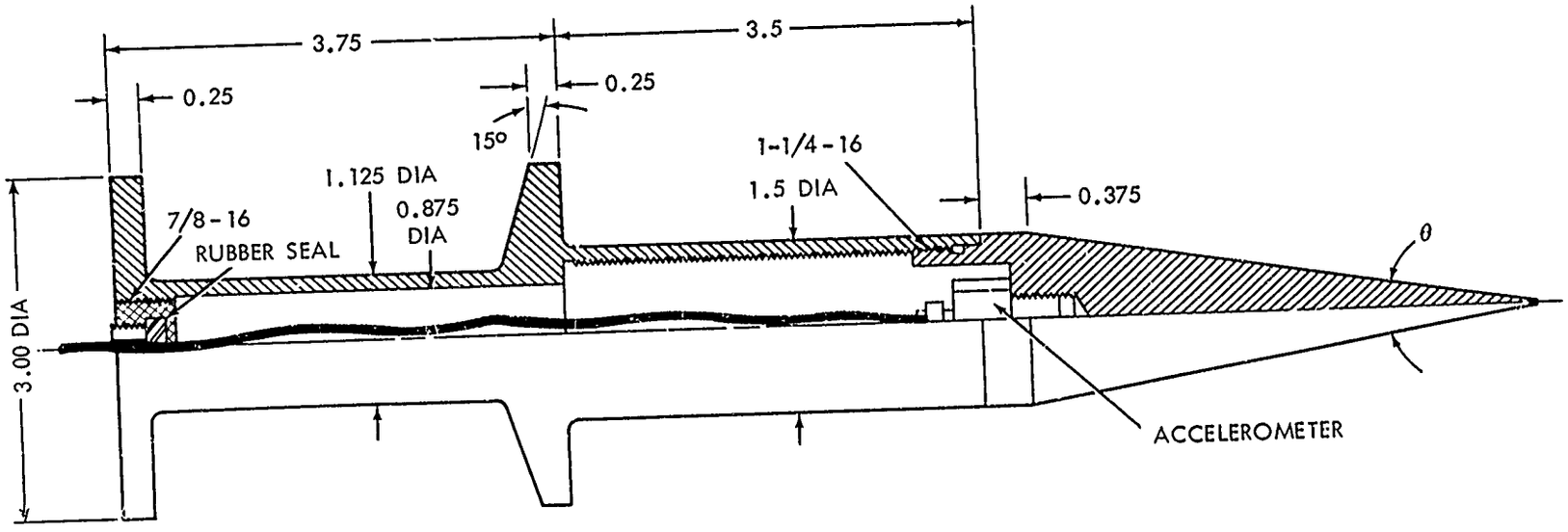

CONE ANGLE θ	WEIGHT GRAMS
10	643
15	572
20	538

FIG. B-1 DRAG PLATE MODEL - 10, 15, and 20° CONE ANGLES

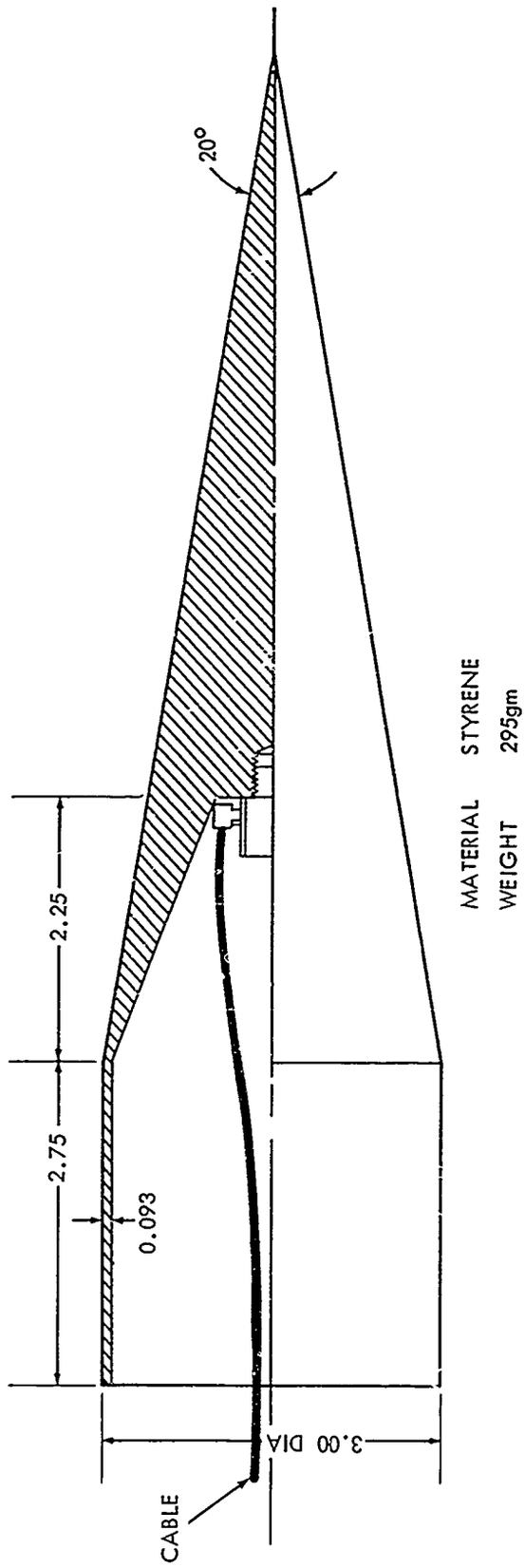

FIG. B-2 LIGHT WEIGHT 20° MODEL

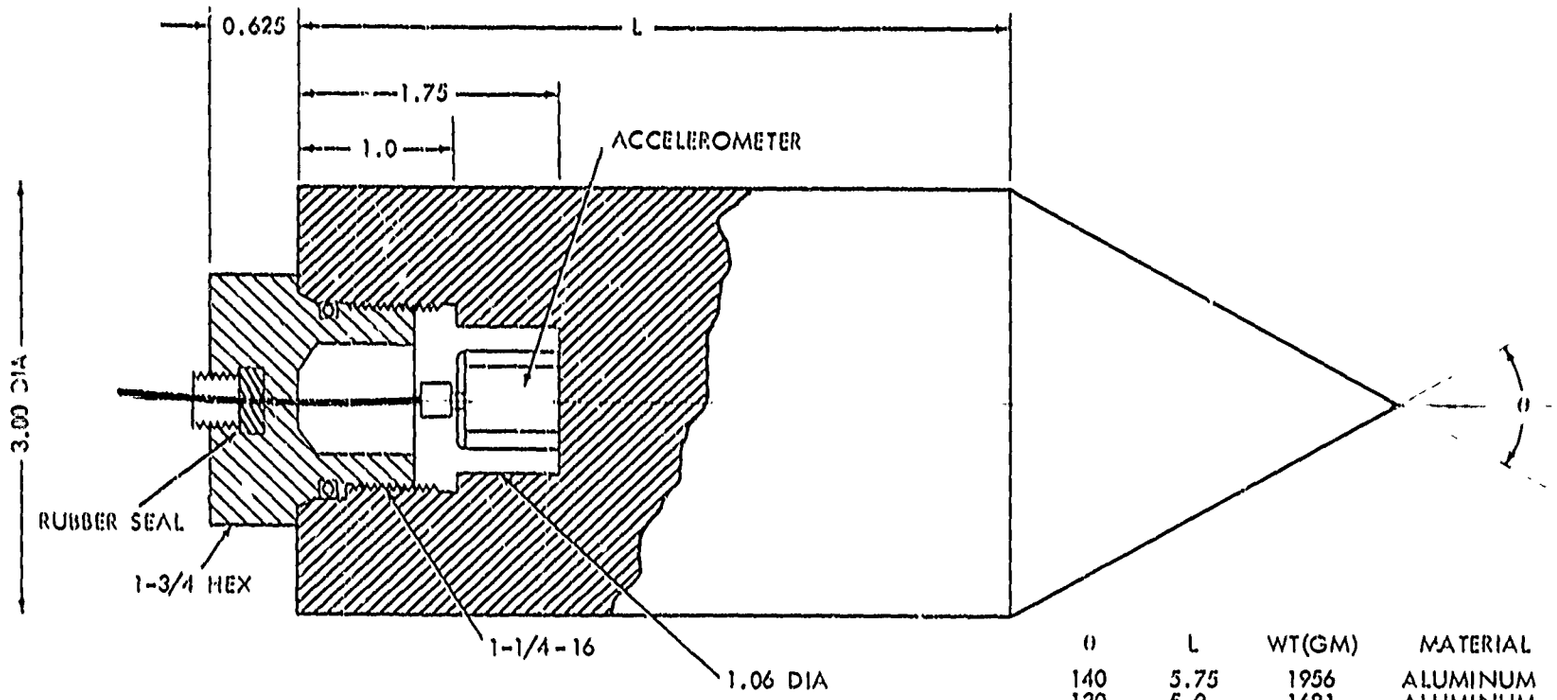

θ	L	WT(GM)	MATERIAL
140	5.75	1956	ALUMINUM
120	5.0	1681	ALUMINUM
190	4.75	1676	ALUMINUM
90	10.0	9387	STEEL
60	4.75	1829	ALUMINUM
45	4.75	1922	ALUMINUM
30	4.75	2136	ALUMINUM
20	4.75	2459	ALUMINUM

FIG. B-3 NORMAL WEIGHT MODELS 20 THROUGH 140° CONE ANGLES

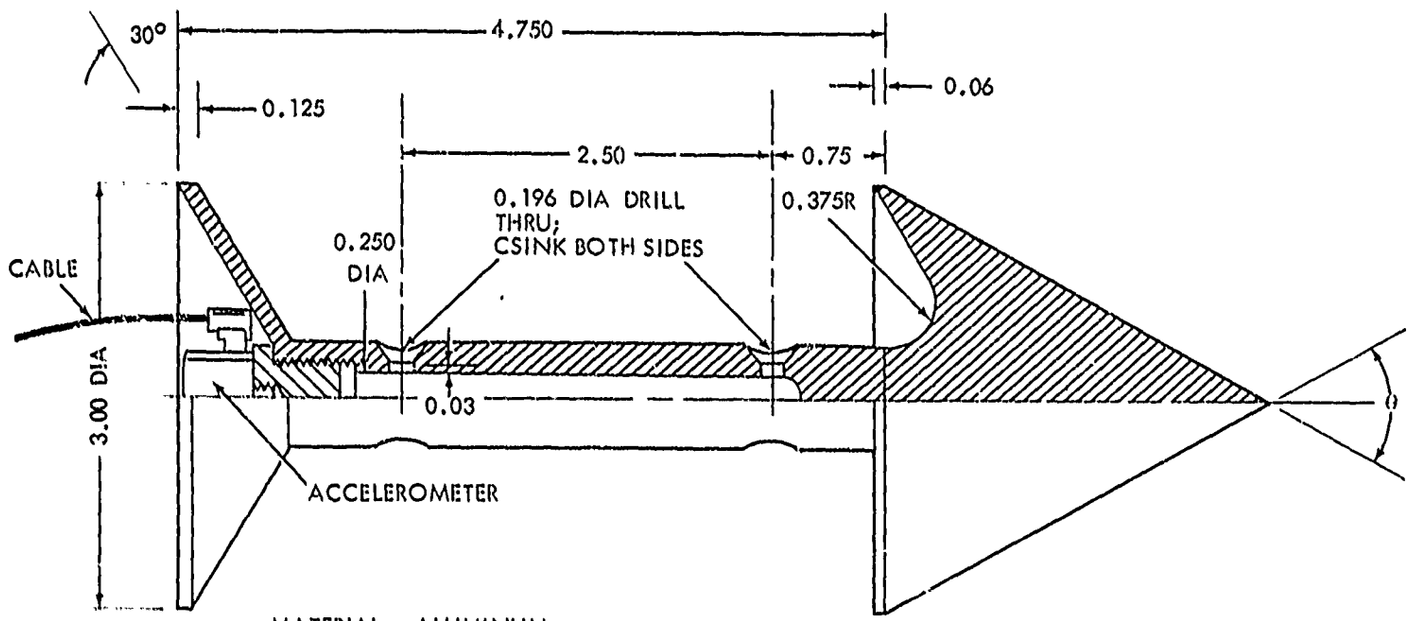

MATERIAL:	ALUMINUM
θ	WEIGHT
45	482 gm
60	379 gm
90	284 gm

FIG. B-4 G LINT MODELS 45, 60, and 90° CONE ANGLES

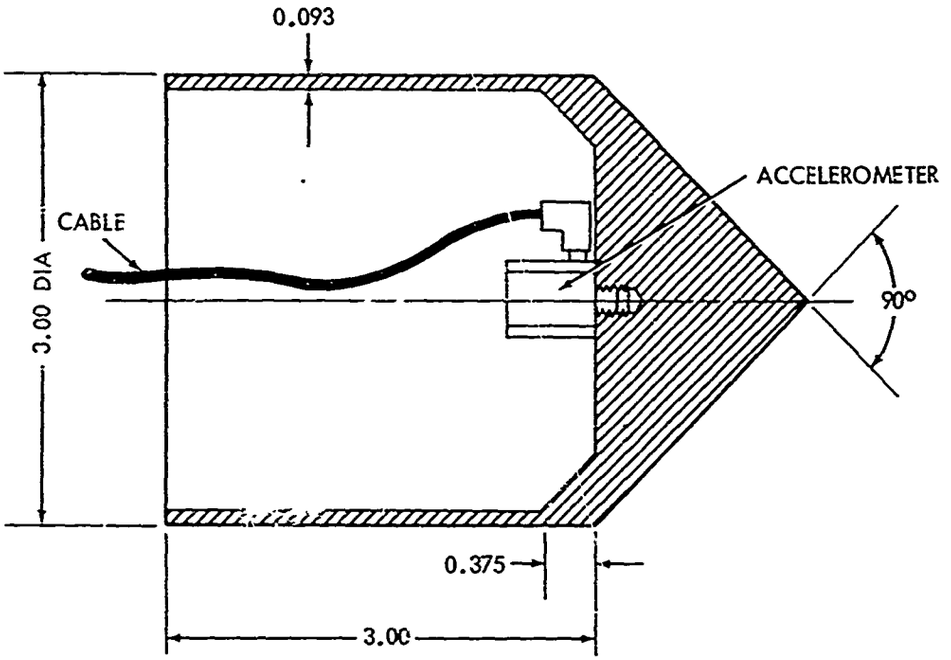

MATERIAL: HIGH IMPACT PLASTIC
WEIGHT: 150 GRAMS

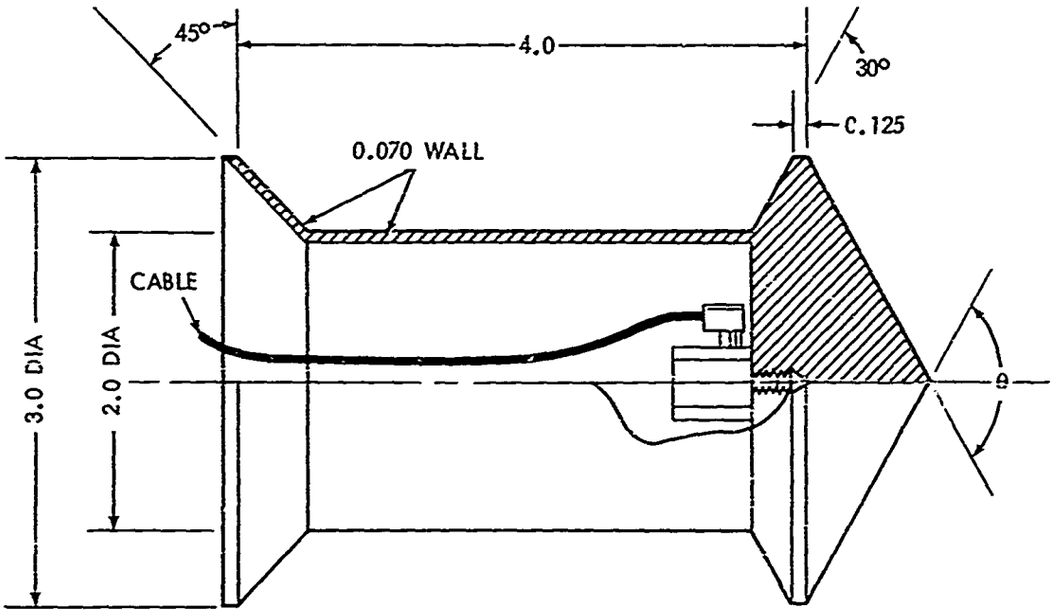

θ	MATERIAL	WT.
120°	STYRENE	128 GRAMS
120°	ALUMINUM	287 GRAMS
140°	ALUMINUM	251 GRAMS

FIG. B-6 LIGHT WEIGHT MODELS 90, 120, and 140° CONE ANGLES

APPENDIX C

In this appendix are numerical values obtained for each test in this series. Also included are plots of average values of total drag coefficient and added mass versus depths for several cone angles.

The following terms have not been previously defined, at least as used in these tables.

added mass coefficient k in $m = \rho k(S/h)^3$

surface heave - cone length minus computer depth

residuals - sum of the square of the residuals resulting from the least square fit of mass constant (total). The number in parentheses is the number of data points used in the least square fit. The average residual is the square of the arithmetic average. The percent residual is 100 (average residual/average total mass constant).

Cd(f) - the amount of Cd delegated to skin friction

Cd ratio - $\frac{Cd - Cd(f)}{Cd}$

In those cases where the tabulated number is not dimensionless, the property listed is for a 3-inch-diameter body except for 10- and 15-degree cones where the values listed appoint a shot number relating to 1.5-inch diameter.

Table C-1. SUMMARY OF CONE DATA

Cone angle	Number of tests	C_D	Total added mass constant	Added mass (gm)	Added mass coefficient	Penetration Ratio Computer % depth	Penetration Ratio Measured % depth	Surface heave
10	4	.02205	.1303	.1750	.003	103.7	105.5	-.634
15	2	.04266	.1892	.3264	.006	105.7	-	-.649
20	10	.0697	.2860	1.772	.032	94.28	96.27	.486
30	8	.1277	.3318	.5683	.010	90.59	88.87	.527
45	14	.2858	.4915	3.115	.056	88.57	86.16	.414
60	13	.4607	.6209	5.636	.102	85.74	84.14	.370
90	26	1.175	1.027	17.92	.324	80.2	80.6	.297
120	32	2.840	1.546	30.13	.545	76.34	75.95	.205
140	9	5.547	2.018	36.23	.655	71.53	68.88	.155

Table C-2. 10-DEGREE TOTAL-ANGLE CONES

Shot number	Weight (gm)	Velocity (ft/sec)	C_D max	Total added mass constant	Residuals	Added mass gm (wt)	Computer depth	Measured depth
1973	643	126	.06165	-	-	-	-	-
1974	643	132	.05789	.3638	1.749-4 (8)	.2852	9.011	9.04
2085	643	144	.05711	.3733	8.365-4 (9)	.1605	8.718	-
2086	643	145	.05314	.2815	8.400-4 (5)	-.2712	8.939	-
Average			.05745	.3395	1.851-3 (22)	.1750	8.889	9.04
Corrected or percent			.02205	.1303	2.71%		103.7%	105.5%

Cot $\theta/2$ = 11.430 Cone length = 8.572 $C_D(f)$ = .0354 C_D ratio = .3838

For corresponding (1) test $\frac{\text{computer depth}}{\text{measured depth}}$ = .9268

Base diameter of all cones tested was 1.5 inches

15-DEGREE TOTAL-ANGLE CONES

Shot number	Weight (gm)	Velocity (ft/sec)	C_D max	Total added mass constant	Residuals	Added mass gm (wt)	Computer depth	Measured depth
1971	572	114.8	.06225	.2526	1.176-4 (8)	.1807	6.196	-
1972	572	121.5	.07021	.3348	2.059-4 (7)	.4721	5.853	-
Average			.06621	.2937	3.235-4 (15)	.3264	6.025	-
Corrected or percent			.04266	.1892	1.67%	2.575	105.7%	-

Cot $\theta/2$ = 7.5958 Cone length = 5.696 $C_D(f)$ = .02355 C_D ratio = .6443

No measured depths possible

Base diameter of all cones tested was 1.5 inches

Table C-3. 20-DEGREE TOTAL-ANGLE CONES

Shot number	Weight (gm)	Velocity (ft/sec)	C_D max	Total added mass constant	Residuals	Added mass gm	Computer depth	Measured depth
2001	295	13.64	.08165	.4012	8.146-3 (7)	1.112	7.374	-
2013	2459	16.36	.09126	.4858	6.588-3 (9)	3.199	8.524	-
1902	2459	43.2	.09198	.4314	7.615-4 (4)	2.078	7.267	8.026
1904	2459	69.6	.08534	.3141	1.350-5 (4)	.1640	7.765	7.890
1905	2459	72.6	.07946	.2715	6.768-5 (6)	-.3771	8.234	-
1914	538*	95.0	.08448	.3145	1.613-3 (7)	.08356	7.766	8.240
1915	538*	125.3	.09729	.3459	1.210-3 (7)	3.851	8.417	8.230
1916	538*	169.9	.08307	.2855	6.624-5 (5)	-.1511	8.049	8.560
1976	538*	204.	.09547	.3273	9.8522-4 (9)	4.564	8.948	-
1977	538*	258.2	.08204	.4049	4.929-3 (9)	3.196	7.840	-
Average			.08729	.3582	2.248-2 (67)	1.772	8.018	8.190
Corrected or percent			.0697	.2860	5.11%		94.28%	96.27%

Cot $\theta/2$ = 5.671 Cone length = 8.507 $C_D(f)$ = .01758 C_D ratio = .7985

For corresponding (5) tests $\frac{\text{computer depth}}{\text{measured depth}}$ = .9588

*1.5 Dia Cone.

Table C-4. 30-DEGREE TOTAL-ANGLE CONES

Shot number	Weight (gm)	Velocity (ft/sec)	C_D max	Total added mass constant	Residuals	Added mass gm	Computer depth	Measured depth
1892	2136	19.86	.1384	.3850	7.329-3 (13)	-	5.113	-
1890	2136	20.87	.1327	.3677	2.286-3 (9)	-.1726	4.844	4.932
1888	2136	22.2	.1351	.4317	3.898-3 (11)	.1240	4.552	4.927
1889	2136	22.2	.1431	.3308	5.400-4 (12)	.7331	5.252	4.932
1893	2136	33.6	.1362	.3162	5.185-5 (5)	.2462	5.319	5.158
1894	2136	42.3	.1433	.4020	2.328-3 (5)	1.263	4.894	-
1895	2136	61.65	.1491	.2945	2.417-3 (3)	1.475	5.656	4.926
1896	2136	91.5	.1367	.3669	2.481-5 (3)	.3097	4.943	-
Average			.1393	.3619	1.83-2 (61)	.5683	5.072	4.975
Corrected or percent			.1277	.3318	4.78%		90.59%	88.87%

Cot $\theta/2$ = 3.732 Cone length = 5.598 $C_D(f)$ = .0116 C_D ratio = .9167

For corresponding (5) tests $\frac{\text{computer depth}}{\text{measured depth}} = 1.0299$

Table C-5. Total Drag Coefficient and Added Mass
10-, 15-, 20- and 30-Degree Total-Angle Cones

Shot No.	Cone Angle (degrees)	Distance* .32	.16	0	.16	.32	.8	2	4	8
2085	10	.056	.057	.057	.057	.057	.057	.056		
2086	10	.052	.052	.053	.053	.053	.053	.0511		
1972	15	.070	.070	.070	.070	.070	.070	.068		
2013	20	-	.101	.103	.103	.102	.100			
1977	20	.082	.820	.082	.082	.082	.081	.079		
1894	30	-	.138	.143	.143	.142	.141	.138	.135	.131
				Added Mass Grams						
2085	10	1.28	1.28	1.28	1.28	1.28	1.28	1.30		
2086	10	-2.1	-2.2	-2.2	-2.2	-2.2	-2.2	-2.5		
1972	15	3.68	3.76	3.76	3.84	3.84	4.0	4.25		
2013	20	-	.59	.61	.63	.64	.67			
1917	20	3.2	3.2	3.2	3.12	3.12	2.96	2.48		
1894	30	-	1.22	1.26	1.27	1.27	1.26	1.20	.89	-.46

*Distance measured from depth of maximum total drag coefficient

Cone Angle	C_{ds}
.0	.0595
15	.0684
20	.0866
30	.141

Table C-6. 45-DEGREE TOTAL-ANGLE CONES

Shot number	Weight (gm)	Velocity (ft/sec)	C_D max	Total added mass constant	Residuals	Added mass gm	Computer depth	Measured depth
2438	482	12.80	.3040	.4896	5.735-3 (10)	2.806	3.182	-
2439	482	12.86	.3103	.5119	1.076-2 (10)	4.043	3.256	3.132
2337	482	13.10	.3098	.6924	4.192-2 (9)	5.550	2.988	-
2440	482	13.32	.3135	.4442	1.295-2 (10)	3.164	3.356	-
1661	1922	18.31	.2907	.4510	2.493-3 (5)	3.461	3.399	-
1663	1922	21.05	.2729	.5222	4.369-4 (5)	2.179	3.085	3.073
1662	1922	21.5	.3005	.3885	6.203-3 (9)	3.495	3.614	3.210
1664	1922	23.20	.2875	.4554	5.316-4 (4)	2.322	3.281	3.073
1675	1922	36.90	.2922	.4986	7.983-4 (9)	3.027	3.195	3.282
1676	1922	39.02	.3126	.5445	3.044-3 (10)	4.159	3.153	3.072
1677	1922	70.56	.2771	.5568	1.459-4 (4)	2.246	2.978	-
1679	1922	79.92	.2768	.4909	6.488-4 (8)	2.057	3.145	3.138
1680	1922	88.5	.2688	.5125	6.588-4 (13)	2.051	3.084	3.100
1681	1922	132.5	.2892	.5033	7.357-5 (6)	3.048	3.194	3.003
Average			.2933	.5044	8.067-2(110)	3.115	3.208	3.120
Corrected or percent			.2858	.4915	5.36%		88.57%	86.16%

Cot $\theta/2$ = 2.414 Cone length = 3.621 $C_D(f)$ = .0075 C_D ratio = .9744

For corresponding (9) tests $\frac{\text{computer depth}}{\text{measured depth}} = 1.032$

Table C-7. Total Drag Coefficient and Added Mass for 45-Degree Cone
$Cd_s = .257$

Shot No \ Depth	Total Drag Coefficient										
	3.128	3.168	3.208	3.248	3.328	3.408	3.608	4.208	5.208	6.208	9.208
2438	.295	.300	.304	.304	.301	.292	.270	.223	.188		
2439	.301	.305	.310	.309	.308	.306	.302	.275	.246	.241	
2437	.299	.305	.310	.309	.307	.304	.292				
2440	.304	.309	.314	.313	.308	.304	.291	.259	.235		
1663	.264	.268	.273	.270	.264	.258	.245	.218	.179		
1662	.293	.297	.300	.298	.294	.290	.281	.261	.240	.228	.198
1664	.276	.281	.288	.284	.276	.269	.253	.221	.191	.165	
1675	.288	.291	.292	.292	.289	.283	.270	.250	.219		
1677	.274	.276	.277	.275	.271	.267	.258	.237	.221	.205	.181
1680	.265	.267	.269	.268	.265	.260	.250	.227	.207	.197	
1681	.284	.287	.289	.288	.286	.283	.274	.254	.242	.235	.224
Average	.285	.290	.293	.291	.288	.283	.272	.244	.218	.214	.206
	Average Added Mass (Grams)										
	2.90	2.99	3.08	3.16	3.31	3.44	3.68	4.31	4.44		

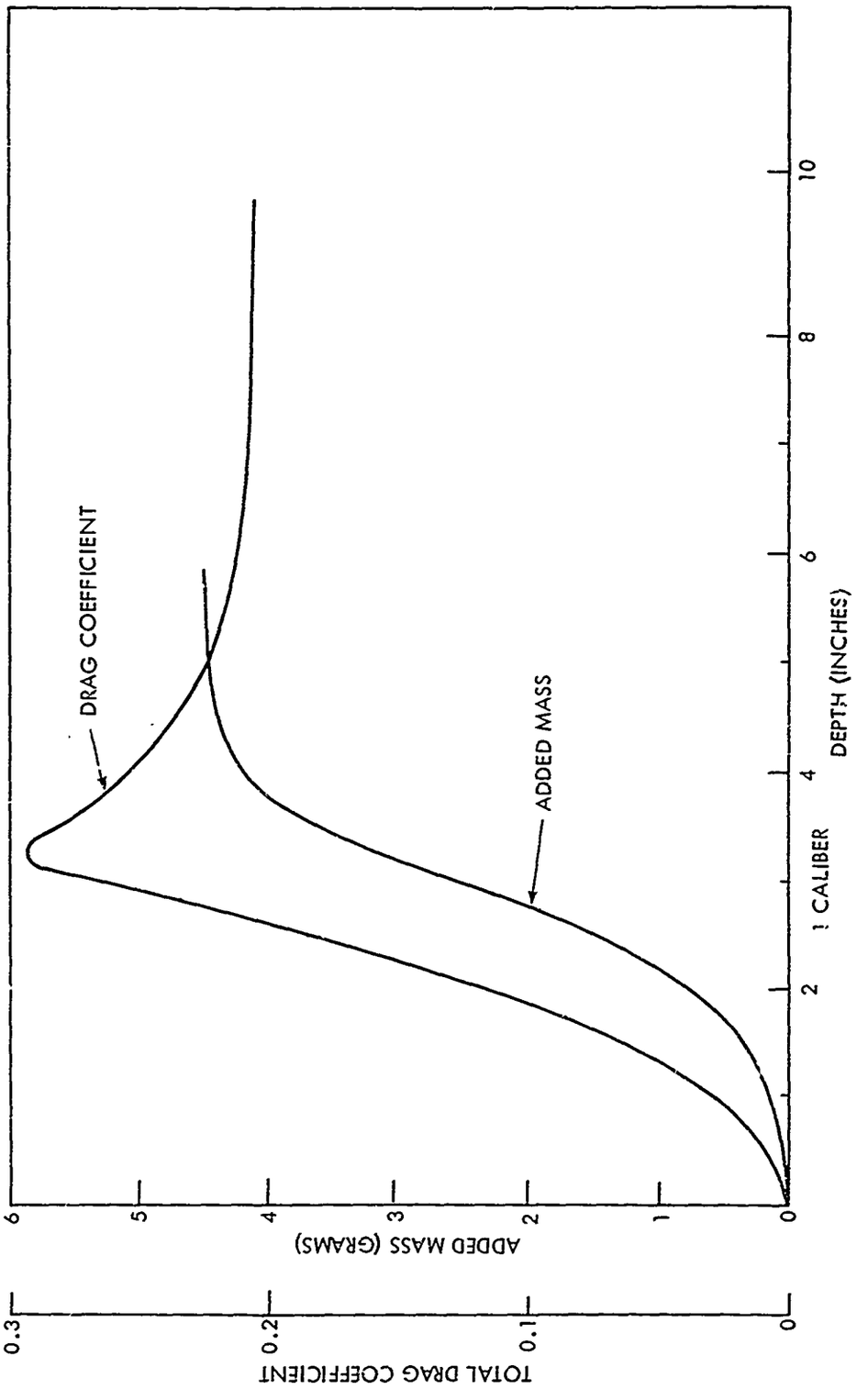

FIG C-1 AVERAGE TOTAL DRAG COEFFICIENT AND ADDED MASS vs DEPTH FOR 45° CONES

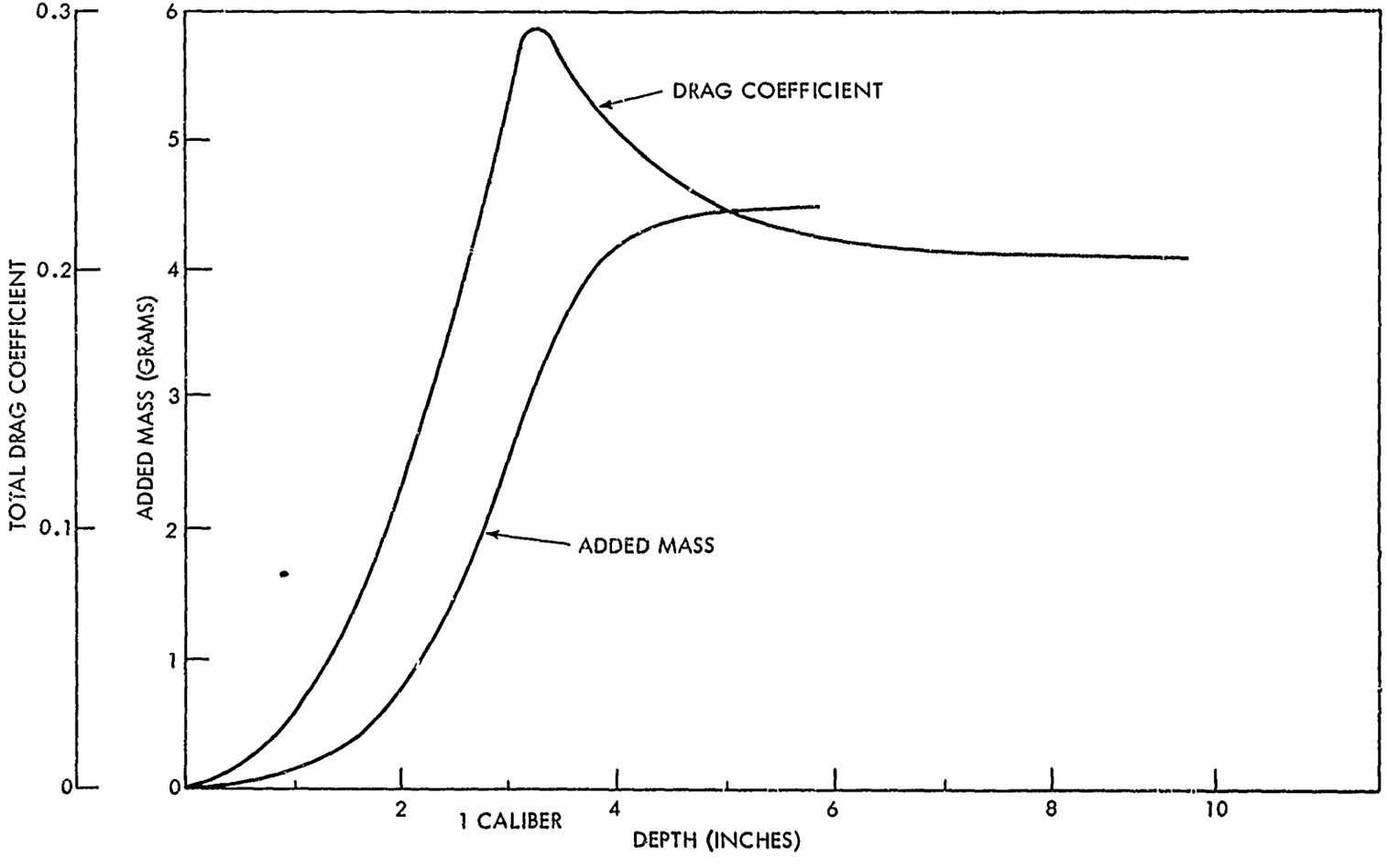

FIG C-1 AVERAGE TOTAL DRAG COEFFICIENT AND ADDED MASS vs DEPTH FOR 45° CONES

Table C-9. Total Drag Coefficient and Added Mass for 60-Degree Cone
$Cd_s = .365$

Total Drag Coefficient

Shot No. \ Depth	2.028	2.148	2.228	2.268	2.308	2.348	2.428	2.628	3.228	4.228	5.228
1954	.382	.413	.430	.424	.417	.412	.399	.341	.314	.279	
2430	.414	.452	.463	.461	.454	.445	.428	.396	.354		
2428	.402	.449	.461	.461	.452	.442	.423	.373			
1953	.391	.420	.439	.433	.467	.420	.408	.375	.323	.297	.231
2429	.454	.483	.489	.482	.475	.465	.445	.409	.357		
1689	.396	.456	.510	.474	.446	.433	.416	.378	.318	.273	
1688	.427	.459	.474	.471	.467	.464	.456	.436	.399		
1687	.395	.418	.427	.423	.419	.415	.407	.382	.323	.279	.249
1691	.402	.446	.476	.473	.469	.462	.446	.398	.342		
1690	.406	.454	.479	.473	.465	.457	.435	.386	.327	.293	
1693	.434	.471	.483	.480	.474	.468	.450	.417	.368	.338	.323
1694	.433	.461	.473	.465	.458	.450	.434	.402	.361	.335	.322
Average	.409	.448	.467	.460	.455	.444	.429	.391	.344		

Average Added Mass (Grams)

5.27	5.52	5.76	5.99	6.20	6.38	6.73	7.28	7.52	7.01

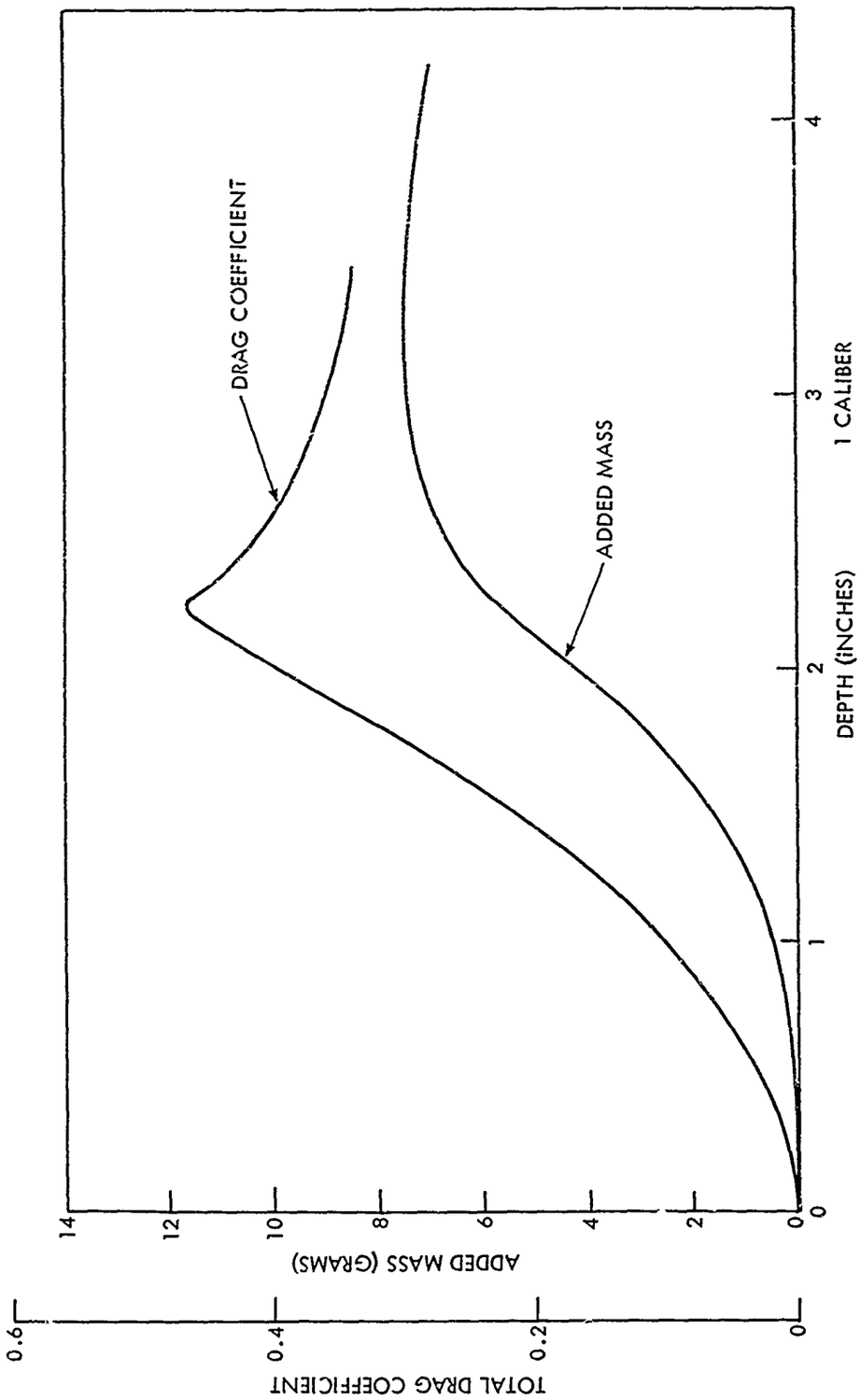

FIG. C-2 AVERAGE TOTAL DRAG COEFFICIENT AND ADDED MASS vs DEPTH FOR 60° CONES

Table C-10. 90-DEGREE TOTAL-ANGLE CONES

Shot number	Weight (gm)	Velocity (ft/sec)	C_D max	Total added mass constant	Residuals	Added mass gm	Computer depth	Measured depth
2435	150	11.57	1.133	.9880	7.268-3 (14)	18.34	1.241	1.197
2436	150	12.96	1.204	1.163	5.052-3 (12)	18.33	1.163	-
2432	284	13.02	1.175	.9916	5.628-3 (10)	21.56	1.289	-
2434	150	13.57	1.167	1.109	4.600-3 (14)	17.20	1.161	-
2431	284	13.59	1.208	1.032	8.753-3 (10)	20.33	1.250	-
2009	1676	16.12	1.224	1.004	6.967-6 (3)	19.36	1.243	1.223
2007	1676	16.45	1.212	1.044	5.479-4 (11)	17.80	1.203	1.223
2005	1676	16.5	1.159	.9598	1.004-3 (7)	20.18	1.285	1.209
2006	1676	16.7	1.214	.9051	6.537-3 (7)	19.00	1.282	1.210
2450	9387	21.64	1.235	1.149	3.655-4 (7)	18.42	1.166	-
2449	9387	21.90	1.209	1.057	1.811-4 (5)	18.85	1.203	-
2448	9387	22.32	1.204	.8930	5.945-3 (8)	18.96	1.280	-
1660	1676	23.97	1.119	1.064	2.353-3 (7)	15.48	1.154	1.171
1659	1676	25.90	1.116	.9868	7.530-3 (9)	14.89	1.174	1.186
31203	1576	26.44	1.174	.9371	8.122-4 (9)	18.84	1.270	1.199
1912	9489	28.15	1.166	.9060	3.060-4 (6)	19.90	1.317	-
1652	1676	45.15	1.198	1.118	3.216-4 (3)	17.96	1.174	-
1651	1676	74.5	1.150	1.034	2.536-3 (6)	16.97	1.194	1.145
1650	1676	88.86	1.169	.9953	1.081-3 (4)	16.91	1.196	1.250
1649	1676	96.0	1.158	1.232	4.608-3 (4)	14.48	1.069	-
1653	1676	145.3	1.142	.9227	1.141-2 (9)	13.86	1.189	1.296
1964	1676	146.0	1.211	.9084	7.978-4 (9)	18.64	1.280	-
1917	1676	154.3	1.156	1.229	4.996-3 (3)	18.94	1.135	1.203
1965	1676	155.7	1.208	1.019	1.093-3 (8)	18.16	1.216	-
1654	1676	169.23	1.148	1.007	2.860-4 (5)	15.82	1.179	-
1918	1676	190.0	1.165	1.215	8.936-3 (11)	16.68	1.124	-
Average			1.178	1.0299	.1321 (201)	17.92	1.203	1.209
Corrected or percent			1.175	1.027	2.49%		80.20%	80.60%

Cot $\theta/2$ = 1.000 Cone length = 1.5 $C_D(f)$ = .0031 C_D ratio = .997

For corresponding (12) tests $\frac{\text{computer depth}}{\text{measured depth}}$ = 1.0037

Table C-11. Total Drag Coefficient and Added Mass for 90-Degree Cone
$Cd_s = .497$

Shot No. \ Depth	Total Drag Coefficient										
	1.123	1.163	1.203	1.243	1.283	1.323	1.403	1.603	2.203	3.203	4.203
2435	1.075	1.116	1.133	1.083	1.026	.971	.861	.727	.594	.438	.303
2436	1.129	1.183	1.204	1.168	1.099	1.009	.891	.740	.580	.457	
2432	1.159	1.180	1.175	1.082	1.016	.953	.868	.743	.650	.586	.534
2434	1.077	1.143	1.166	1.150	1.084	1.052	.930	.740	.588		
2431	1.136	1.184	1.208	1.15	1.166	1.178	.915	.776	.646	.595	
2009	1.104	1.164	1.224	1.150	1.082	1.020	.923	.776	.643	.587	.547
2007	1.066	1.135	1.212	1.182	1.137	1.076					
2005	1.106	1.137	1.159	1.126	1.066	.990	.879	.733	.592	.511	
2006	1.110	1.166	1.214	1.180	1.109	1.035	.921	.776			
2450	1.130	1.188	1.235	1.193	1.109	1.031	.897	.733	.548	.469	
2449	1.102	1.159	1.209	1.158	1.098	1.015	.887	.734	.564	.527	.47[illegible]
2448	1.107	1.163	1.204	1.177	1.085	1.007	.940	.800	607	.565	
1660	1.019	1.071	1.119	1.058	.998	.932	.821	.679	.533	.451	.402
31203	1.087	1.136	1.174	1.128	1.069	.990	.877	.748	.530	.417	.360
1912	1.056	1.109	1.166	1.101	1.041	.992	.911	.750	.643	.600	.575
1652	1.069	1.134	1.198	1.121	1.040	.953	.809	.719	.537	.463	.421
1651	1.052	1.104	1.150	1.081	1.007	.936	.831	.685	.551	.480	
1650	1.053	1.112	1.169	1.112	1.046	.983	.870	.727	.574	.505	.470
1649	.962	1.052	1.158	1.123	1.085	1.040	.930	.757	.582	.500	.456
1653	.927	.989	1.142	1.073	1.006	.938	.820	.673	.530	.448	.430
1964	1.092	1.155	1.211	1.163	1.109	1.022	.882	.751	.609	.540	.510
1917	1.109	1.139	1.156	1.103	1.047	.979	.845	.591	.535	.503	
1654	1.025	1.087	1.148	1.076	1.009	.949	.841	.685	.561	.490	.471
1918	1.048	1.106	1.165	1.180	1.153	1.082	.895	.763	.619	.554	.520
Average	1.075	1.130	1.179	1.130	1.070	1.005	.880	.730	.584	.487	.466
	Average Added Mass (Grams)										
	15.0	16.5	18.0	19.6	20.9	22.2	24.2	27.8	33.0	35.8	39.7

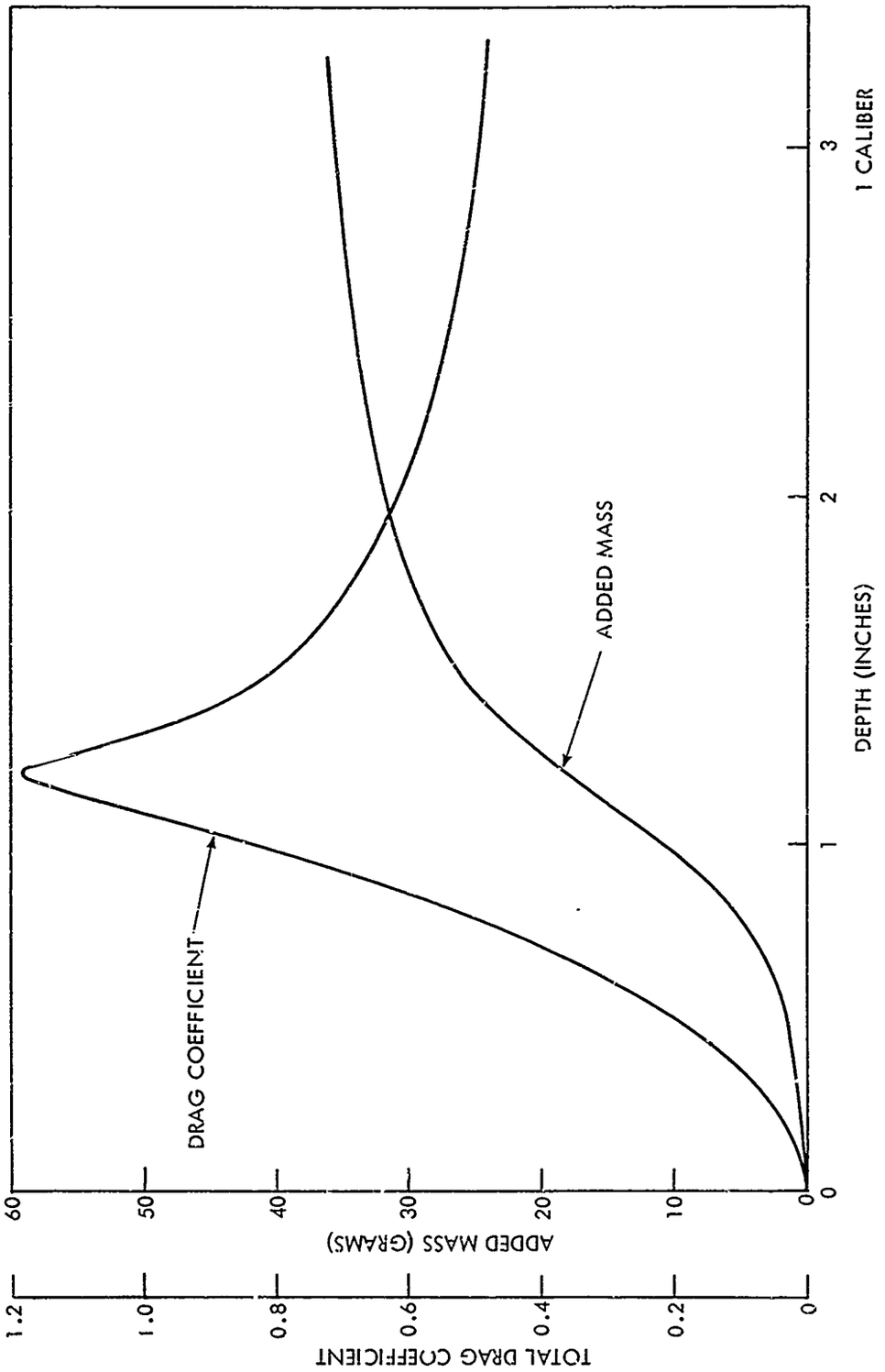

FIG. C-3 AVERAGE TOTAL DRAG COEFFICIENT AND ADDED MASS vs DEPTH FOR 90° CONES

Table C-12. 120-DEGREE TOTAL-ANGLE CONES

Shot number	Weight (gm)	Velocity (ft/sec)	C_D max	Total added mass constant	Residuals	Added mass gm	Computer depth	Measured depth
21402	128	10.5	2.696	1.651	9.656-3 (12)	27.89	.6327	-
2060	128	11.10	2.648	1.552	3.620-2 (9)	28.43	.6525	-
2062	128	11.25	2.847	1.525	1.431-2 (10)	34.09	.6886	.682
2061	128	12.2	2.657	1.530	6.652-3 (9)	29.63	.6648	.681
2030	1678	13.137	3.091	1.203	4.705-2 (7)	34.67	.7465	-
2032	1678	13.457	2.879	1.347	2.897-3 (7)	30.64	.6912	-
2033	1789	13.64	3.003	1.573	3.083-2 (7)	29.99	.6543	-
2034	1789	13.6	3.144	1.618	5.677-3 (5)	33.47	.6694	-
2002	1789	15.7	2.917	1.502	1.122-3 (10)	33.01	.6870	.680
21403	287	15.79	2.755	1.499	2.216-3 (8)	28.56	.6549	.674
21404	287	15.94	2.639	1.644	.3582 (13)	26.818	.6284	.6558
1995	1681	15.95	2.809	1.513	2.949-3 (10)	29.91	.6648	-
2004	1789	16.17	2.726	1.445	3.253-2 (10)	30.298	.6792	.717
2003	1789	16.185	2.681	1.704	5.378-3 (9)	26.11	.6139	.601
1996	1681	16.2	2.739	1.481	6.463-3 (10)	28.31	.6594	-
1997	1681	16.44	2.699	1.578	2.113-3 (10)	27.69	.6421	.588
21302	1681	19.63	2.885	1.568	4.671-4 (6)	28.98	.6521	-
20606	1681	23.98	2.949	1.853	2.203-2 (5)	26.81	.5933	-
20608	1681	24.11	2.770	1.667	3.498-3 (6)	25.62	.6129	-
21301	1681	24.67	3.013	1.573	2.711-20 (2)	34.48	.6696	-
30402	1681	24.74	3.117	1.790	2.203-3 (10)	31.84	.6346	.593
30401	1681	24.81	3.130	1.614	1.906-2 (11)	33.65	.6621	-
1983	1789	32.46	2.883	1.506	4.066-3 (10)	31.81	.6766	-
1982	1789	47.71	2.900	1.363	1.877-4 (6)	32.27	.7081	.700
1981	1789	67.7	2.913	1.518	7.499-3 (8)	31.97	.6764	-
1970	1796	102.2	2.833	1.351	5.554-3 (11)	32.56	.7096	-
1962	1796	125.7	2.716	1.636	4.351-4 (9)	28.36	.6356	.626
1967	1789	134.5	2.849	1.442	2.238-3 (9)	31.26	.6846	-
1966	1789	142.8	2.759	1.714	7.589 3 (9)	28.07	.6250	-
1969	1796	143.0	2.931	1.644	4.139-2 (9)	31.701	.6557	.694
1968	1728	146.0	2.655	1.288	1.290-3 (8)	28.433	.6934	-
1961	1796	146.5	2.663	1.585	3.455-2 (11)	26.92	.6343	-
Average			2.842	1.546	.6166(276)	30.13	.6611	.6577
Corrected or percent			2.840		3.05%		76.34%	75.95%

Cot $\theta/2$ = .5774 Cone length = .8660 $C_D(f)$ = .0018 C_D ratio not used

For corresponding (12) tests $\frac{\text{computer depth}}{\text{measured depth}} = 1.000$

Table C-13. Total Drag Coefficient and Added Mass for 120-Degree Cone
$Cd_s = .596$

Total Drag Coefficient

Shot No \ Depth	.581	.621	.661	.701	.741	.781	.861	1.061	1.661	2.661	3.661
21402	2.176	2.467	2.696	2.487	2.164	1.766	1.322	.949	.626		
2062	2.411	2.673	2.846	2.183	1.739	1.525	1.250	1.071			
2061	2.203	2.461	2.657	2.240	1.750	1.443	1.157	.885	.618		
2030	2.454	2.782	3.091	2.515	1.928	.896					
2032	2.234	2.577	2.879	2.305	1.813	1.549	.891				
2034	2.360	2.677	3.144	2.613	1.880	1.589	1.295				
2002	2.407	2.673	2.917	2.672	2.337	1.910					
21403	2.186	2.467	2.755	2.164	1.674	1.398	1.161	.950	.813	.804	
2004	2.236	2.521	2.726	2.221	1.759	1.503	1.293	1.082	.872		
2003	2.113	2.402	2.681	2.573	2.405	2.181	1.669	1.249			
1996	2.181	2.471	2.739	2.526	2.113	1.768	1.316				
1997	2.147	2.418	2.699	2.485	2.153	1.842	1.416	1.054	.820		
1983	2.309	2.585	2.883	2.523	2.200	1.914	1.449	.853	.748	.708	
1982	2.355	2.653	2.901	2.202	1.832	1.562	1.339	1.046	.807	.864	
1981	2.384	2.666	2.913	2.089	1.750	1.520	1.266	1.006	.787	.694	.639
1970	2.349	2.626	2.883	2.027	1.666	1.476	1.261	1.034	.822	.716	.680
1967	2.290	2.574	2.849	2.484	2.157	1.868	1.403	1.103	.875	.759	.713
1969	2.299	2.654	2.931	2.243	1.730	1.488	1.288	1.084	.841	.758	.730
1968	2.128	2.392	2.655	2.269	1.835	1.496	1.199	.964	.740	.644	.600
2033	2.231	2.585	3.003	2.582	1.873						
Average	2.273	2.566	2.842	2.370	1.938	1.615	1.293	1.024	.781	.743	.673

Average Added Mass (Grams)

21.2	25.8	30.7	35.4	38.9	41.5	45.5	51.8	61.6	72.8	79.7

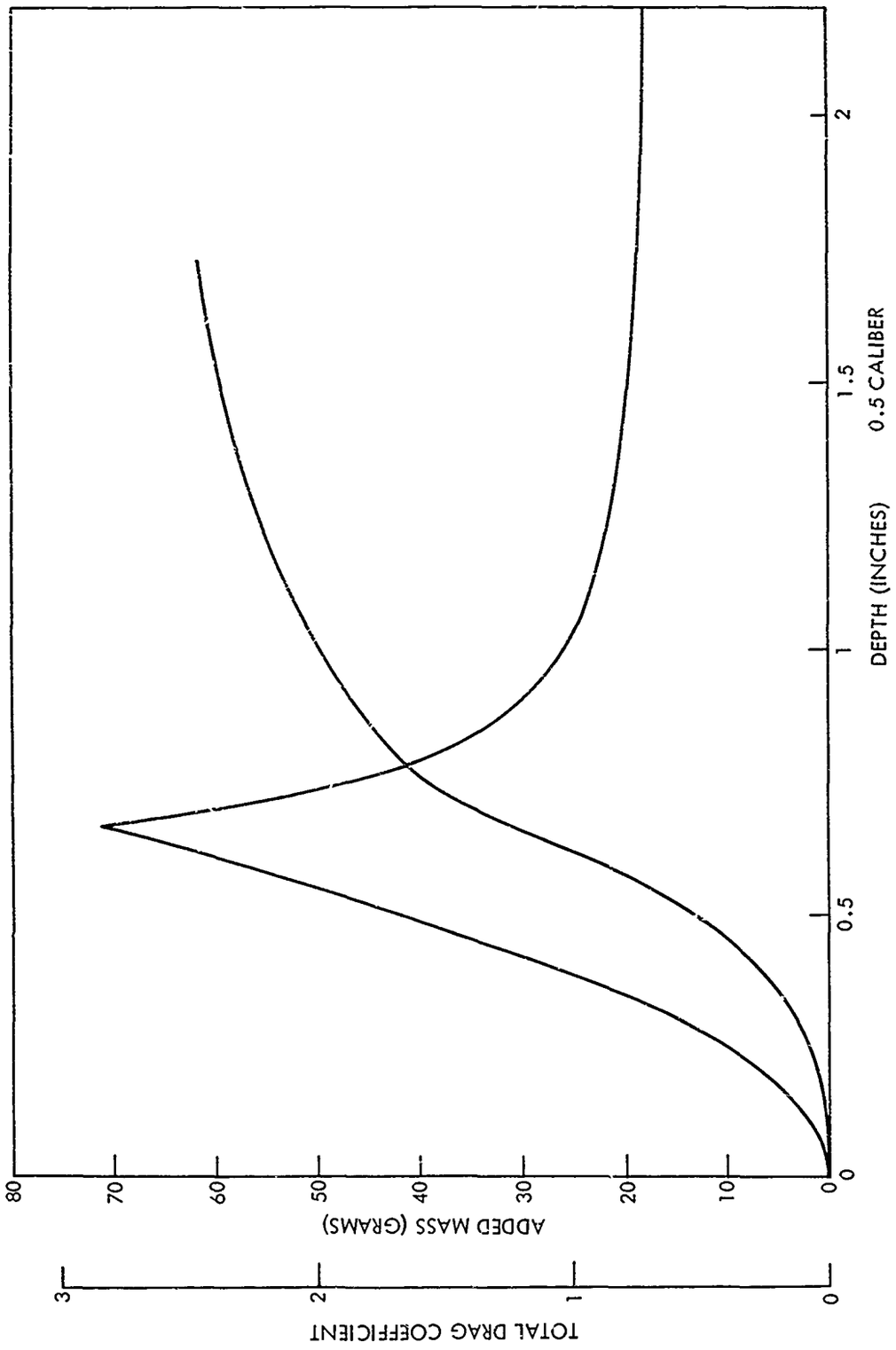

FIG. C-4 AVERAGE TOTAL DRAG COEFFICIENT AND ADDED MASS vs DEPTH FOR 120° CONES

Table C-14. 140-DEGREE TOTAL-ANGLE CONES

Shot number	Weight (gm)	Velocity (ft/sec)	C_D max	Total added mass constant	Residuals		Added mass gm	Computer depth	Measured depth
2022	251	12.03	5.288	1.979	3.530-4	(4)	36.41	.3937	.398
21405	251	12.15	5.280	2.034	9.617-4	(6)	35.98	.3899	.362
2023	251	12.69	5.594	1.976	3.963-3	(11)	40.08	.4083	-
2037	1956	13.589	5.401	2.302	.1828	(5)	28.59	.3446	.335
2038	1956	13.7	5.766	1.863	5.447-3	(5)	31.19	.3824	-
2026	1840	13.74	5.697	1.949	1.934-2	(5)	37.89	.3998	.368
2024	1840	14.24	5.483	2.018	2.209-2	(5)	35.94	.3893	.418
2443	1840	23.13	5.678	2.047	2.517-3	(7)	39.59	.4008	-
2442	1840	23.14	5.738	1.998	3.899-3	(7)	40.43	.4066	-
Average			5.547	2.018	.2413	(55)	36.23	.3905	.376
Corrected or percent					3.28%			71.53%	68.88%

Cot $\theta/2$ = .36397 Cone length = .5459 $C_D(f)$ = .0011 C_D ratio not used

For corresponding (5) tests $\frac{\text{computer depth}}{\text{measured depth}} = 1.019$

Table C-15. Total Drag Coefficient and Added Mass for 140-Degree Cone
$Cd_s = .66$

Shot No. \ Depth	Total Drag Coefficient										
	.312	.352	.393	.432	.472	.512	.592	.792	1.392	2.392	3.392
2022	3.42	4.34	5.29	4.09	2.38	1.89	1.44	1.16			
21405	3.40	4.35	5.27	4.36	2.89	2.10	1.62				
2023	3.76	4.63	5.59	3.12	2.14	1.79	1.47	1.16			
2037	2.40	3.92	5.40								
2038	3.93	3.32	5.76	4.46							
2026	3.50	4.46	5.70	3.67	2.38	1.90	1.52	1.31	.909		
2024	3.41	4.41	5.48	4.07	2.65	1.91	1.49	1.16	.876	.729	.658
2443	3.71	4.66	5.67	4.33	2.69	2.12	1.72	1.38			
2442	3.74	4.77	5.74	4.15	2.65	2.11	1.70	1.33			
Average	3.59	4.32	5.54	4.05	2.54	1.97	1.57	1.26	.90	.73	.66
	Average Added Mass (Grams)										
	18.3	25.4	36.2	45.7	51.0	54.5	59.5	68.9	78.0	90.1	91.2

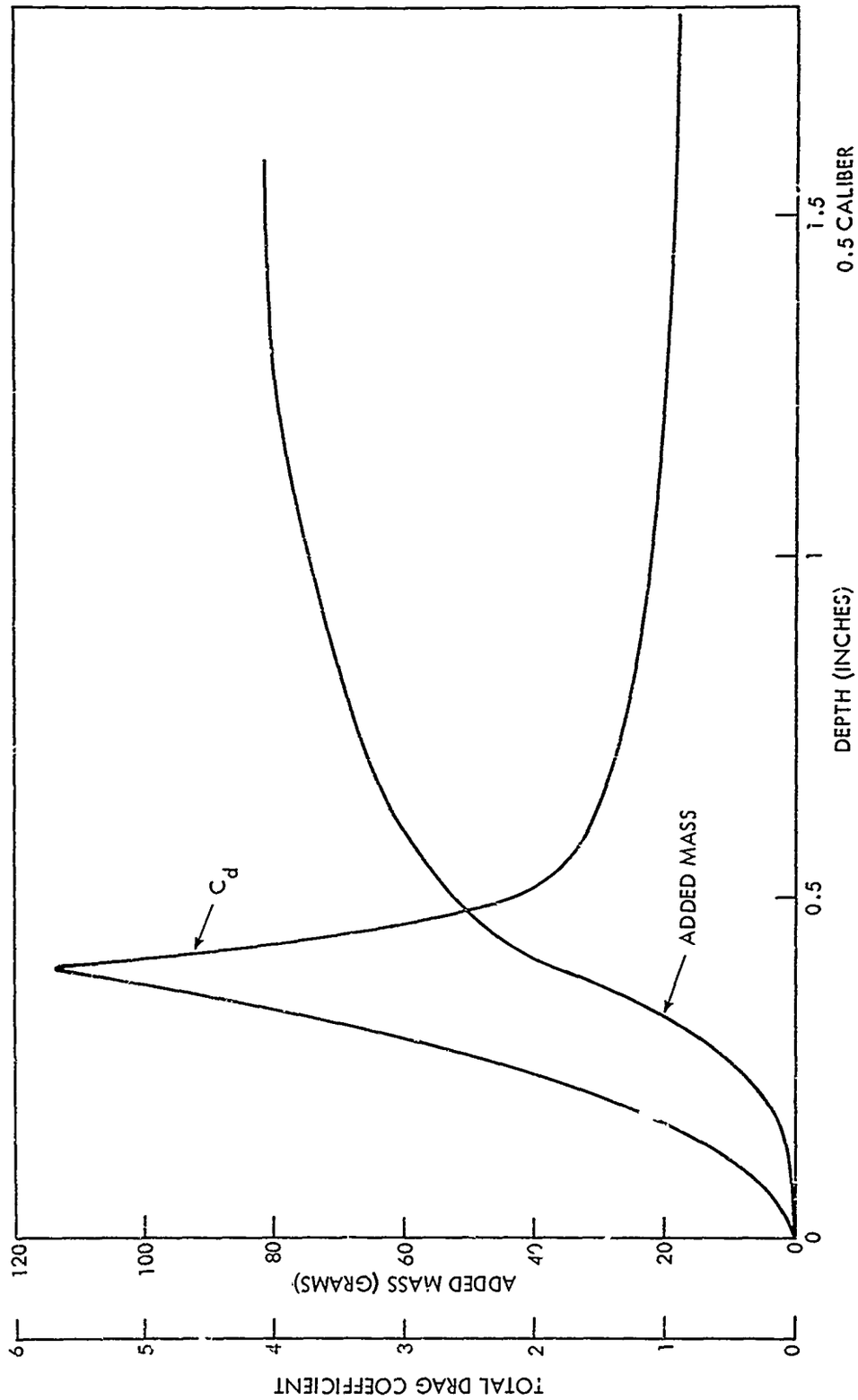

FIG. C-5 AVERAGE TOTAL DRAG COEFFICIENT AND ADDED MASS vs DEPTH FOR 140° CONES

APPENDIX D

This computer program written in BASIC provides the numerical solution to the force equation associated with the water entry of cones. For the sake of simplicity, the drag coefficients and the penetration ratios are required inputs for each run, as is the cone angle. If desired, Cd_{max}, Cds and h may be easily computed internally from polynomial equations in θ. The various sections of the program perform the function as follows:

SUB 500 - reads in data and establishes the depth stations

SUB 700 - computes buoyancy and total drag coefficient for each depth station

SUB 900 - computes added mass for each depth station

SUB 1000 - computes dU/dS based upon previous velocity and integrates to obtain new velocity. The interaction process is stopped when ΔU is sufficiently small

SUB 1200 - computes acceleration

SUB 1500 - prints out

Line 1700 - data input

The data input, in order, consists of: maximum total drag coefficient (Cd); steady-state drag coefficient (Cds); added mass constant (k); and total cone angle (θ) in degrees; base diameter in feet; penetration ratio (h); body weight in pounds; and entry velocity (Uo) in feet per second.

NOTE: Do not forget to include skin friction in maximum total drag coefficient and steady-state drag coefficient.

NOT REPRODUCIBLE

CONE ANGLE = 90.
DIAMETER IN FT = .25
WEIGHT IN LBS = 5

DIST FT	VEL FT/SEC	ACC FT/SEC↑2	DRAG C
0	100	32.2	0
6.66744E-3	99.9964	16.1635	5.23556E-3
1.33349E-2	99.9936	-31.9394	2.09422E-2
2.00023E-2	99.9845	-112.083	.04712
2.66698E-2	99.969	-224.205	8.37689E-2
3.33372E-2	99.9449	-368.189	.130869
4.00046E-2	99.9102	-543.647	.18848
4.66721E-2	99.8627	-750.9	.256542
5.33395E-2	99.8003	-988.964	.335076
6.00069E-2	99.7209	-1257.53	.42408
6.66744E-2	99.6225	-1555.95	.523556
7.33418E-2	99.5031	-1883.44	.633502
8.00093E-2	99.3606	-2239.01	.75392
8.66767E-2	99.1931	-2621.53	.884609
9.33441E-2	98.9987	-3029.66	1.02617
.100012	98.7756	-3461.89	1.176
.106679	98.5567	-2890.91	.990981
.113346	98.3699	-2499.75	.862302
.120014	98.2053	-2229.25	.773184
.126681	98.0561	-2040.13	.710956
.133349	97.9176	-1906.14	.667055
.140016	97.7868	-1809.7	.63569
.146684	97.6616	-1738.98	.612942
.153351	97.5404	-1685.99	.596148
.160019	97.4223	-1645.33	.583499
.166686	97.3066	-1613.33	.573763
.173353	97.1928	-1587.47	.566095
.180021	97.0804	-1566.03	.559916
.186688	96.9693	-1547.84	.554823
.193356	96.8593	-1532.07	.550536
.226693	96.3203	-1474.04	.536045
.26003	95.7959	-1433.52	.527266
.326704	94.7747	-1374.86	.516653

NOT REPRODUCIBLE

CONE ANGLE = 90.
DIAMETER IN FT = 1.8
WEIGHT IN LBS = 18

DIST FT	VEL FT/SEC	ACC FT/SEC+2	DRAG C
0	100	32.2	0
4.800056E-2	99.9369	-198.405	5.235560E-3
9.60111E-2	99.6455	-863.407	2.094222E-2
.144017	98.9193	-1969.07	.04712
.192022	97.5614	-3433.26	8.376892E-2
.240028	95.4101	-5074.05	.130869
.288033	92.3584	-6717.67	.18848
.336039	88.372	-8144.97	.256542
.384044	83.4986	-9163.18	.335076
.43205	77.8659	-9646.34	.42408
.480056	71.6659	-9566.55	.523556
.528061	65.1291	-8991.86	.633502
.576067	58.4947	-8057.64	.75392
.624072	51.9828	-6924.69	.884809
.672078	45.7747	-5741.21	1.02617
.720083	40.0023	-4619.04	1.176
.768089	35.3224	-2841.01	.990981
.816094	31.9717	-1942.21	.862302
.8641	29.3999	-1433.97	.773184
.912106	27.3241	-1121.64	.710956
.960111	25.5859	-916.373	.667055
1.00812	24.091	-773.859	.63569
1.05612	22.7807	-670.416	.612942
1.10413	21.617	-592.598	.596148
1.15213	20.5744	-532.393	.583499
1.20014	19.6352	-484.818	.573763
1.24814	18.7868	-446.651	.566095
1.29615	18.0197	-415.729	.559916
1.34416	17.3265	-390.544	.554823
1.39216	16.7015	-370.011	.550538
1.63219	14.421	-313.53	.536045
1.87222	13.3138	-304.178	.527266
2.35227	13.1687	-345.665	.516853

```
10 DIM S(100),B(100),V(100),M(100),A(100),Z(100)
15 DIM C(100)
20 REM C1=MAXUIM DRAG, C2= STEADY STATE DRAG, K1=ADDED MASS
22 REM CØNSTANT,  A4=CØNE ANGLE , D2=DIAMETER (FT)
24 REM H=PENATRATIØN RATIO, W1=WEIGHT
100 GØ SUB 500
110 GØ SUB 700
115 GØ SUB 900
120 GØ SUB 1000
125 GØ SUB 1200
130 GØ SUB1500
500 READ C1,C2,K1,A4
505 READ D2,H,W1
507 READ V1
510 LET V2=0
515 LET V3=0
520 LET S(1)=0
545 LET A4=A4/(2*57.3)
550 LET A5=.5*D2/TAN(A4)
554 LET A6=A5*H
556 LET D1=A6/15
558 FØR K=2 TØ 30
560 LET S(K)=S(K-1)+D1
562 NEXT K
565 LET S(31)=S(30)+5*D1
570 LET S(32)=S(30)+10*D1
575 LET S(33)=S(30)+20*D1
580 RETURN
700 LET B(1)=0
705 LET C(1)=0
710 FØR K=1 TØ 33
715 LET B(K)=62.4*(3.1416/3)*S(K)↑3*(TAN(A4))↑2
720 IF S(K)<A5 GØ TØ 730
725LET B(K)=62.4*(3.1416/4)*D2↑2*(S(K)-(2/3)*A5)
730 NEXT K
735 FØR K=1 TØ 16
740 LET C(K)=C1*S(K)↑2/A6↑2
745 NEXT K
750 LET R=.5*D2
755 FØR K=17 TØ 33
762 LET C4=.661*((S(K)-S(16))/S(16))
765 LET A9=.3/(1+(S(K)-S(16))/(.5*D2))↑2+EXP(-9*C4)
770 LET C(K)=(C1-C2)*(1/1.3)*A9+C2
780 NEXT K
785 FØR K = 1 TØ 33
787 LET V(K)=V1
789 NEXT K
790 RETURN
900 LET M(1)=0
910 FØR K=1 TØ 16
920 LET M(K)=(62.4/32.2)*K1*S(K)↑3
930 NEXT K
940 FØR K=17 TØ 33
945 LET P=S(K)-S(K-1)
```

```
950 LET M(K)=M(K-1)+((62.4/(4.4)*.7854*D2↑2-(.5*(C(K)+C(K-1))-C2)*P
960 NEXT K
970 RETURN
1000 FOR K=2 TO 33
1010 LET Z(K)=-((62.4/(4.4)*C(K)*.7854*D2↑2*V(K)
1015 LET Z(K)=(Z(K)+(E(K)-W1)/V(K))/((W1/32.2)+M(K))
1020 NEXT K
1030 FOR K= 2 TO 33
1040 LET V(K)=V(K-1)+.5*(Z(K)+Z(K-1))*(S(K)-S(K-1))
1050 NEXT K
1060 LET V5=ABS(V2-V(16))+ABS(V3-V(32))
1070 IF V5<.001 THEN 1110
1080 LET V2=V(16)
1090 LET V3=V(32)
1100 GO TO 1000
1110 RETURN
1200 FOR K =1 TO 33
1210 LET A(K)=-(((62.4/(4.4)*.7854*C(K)*D2↑2*V(K)↑2+E(K)-W1)
1215 LET A(K)=A(K)/((W1/32.2)+M(K))
1220 NEXT K
1230 RETURN
1500 LET AB=2*57.3*A4
1505 PRINT 'CONE ANGLE =     'AB
1510 PRINT 'DIAMETER IN FT ='D2
1520 PRINT 'WEIGHT IN LBS ='W1
1530 PRINT 'DIST','VEL','ACC','DRAG C'
1540 PRINT 'FT','FT/SEC','FT/SEC↑2'
1550 FOR K= 1 TO 33
1560 PRINT S(K),V(K),A(K),C(K)
1570 NEXT K
1700 DATA 1.176,.497,.02,90
1710 DATA -25,.8,5
1720 DATA 100
9999 END
```